SACLANTCEN Memorandum SM - 191

SACLANTCEN Memorandum SM - 191

SACLANTCEN Memorandum SM -191

SACLANT ASW RESEARCH CENTRE MEMORANDUM

MEASUREMENTS OF CORRELATION LOSS AND TIME-SPREADING IN LINEAR FM SWEEPS AND PSEUDO-RANDOM NOISE SIGNALS TRANSMITTED OVER LONG RANGES IN SHALLOW WATER

by

Tor KNUDSEN

DECEMBER 1986

NORTH ATLANTIC TREATY ORGANIZATION

SACLANTCEN
LA SPEZIA, ITALY

Report no. changed (Mar 2006): SM-191-UU

Report no. changed (Mar 2006): SM-191-UU

SACLANTCEN MEMORANDUM SM-191

NORTH ATLANTIC TREATY ORGANIZATION

SACLANT ASW Research Centre
Viale San Bartolomeo 400,
I-19026 San Bartolomeo (SP), Italy.

tel: national 0187 540111
international + 39 187 540111

telex: 271148 SACENT I

MEASUREMENTS OF CORRELATION LOSS AND TIME-SPREADING IN LINEAR FM SWEEPS AND PSEUDO-RANDOM NOISE SIGNALS TRANSMITTED OVER LONG RANGES IN SHALLOW WATER

by

Tor Knudsen

December 1986

This memorandum has been prepared within the SACLANTCEN
Systems Research Division as part of Project 22.

J. MARCHMENT
Division Chief

Abstract

The results of some transmission measurements made in shallow water are described. The ranges were about 15 km, 20 km, and 34 km, and the sound source was either suspended about 10 m above the bottom or was on the bottom in about 60 m of water depth. The signal was received on a vertical string of hydrophones at 10, 20, 40, 80 and 160 m depths. Both linear FM sweeps and pseudo-random noise signals with different time/bandwidth products were transmitted. The centre frequency was 1087.5 Hz. The sound-speed profile was of a very downward refracting type, forcing great interaction with the sea bottom. In the calm weather prevailing, the sound experienced nearly specular reflection from the sea surface. The two shortest ranges were over a hard sandy bottom, resulting in severe multipath propagation that caused acoustic travel times to fluctuate by about 130 ms around their mean. The longest range was over a soft lossy bottom and very little fluctuation in travel time was observed. The loss in processing gain compared with the theoretical gain was generally more severe for the shallow receivers than for the deep receivers, which were situated below a steep gradient in the sound-speed profile. The multipath spread was generally also more severe for the shallow receivers. The pseudo-random noise signals experienced a great increase in processing loss with increasing pulse length, while processing loss for the FM-swept signals showed virtually no increase for pulse lengths of up to 16 s. The transmission loss over the 20 km range was modelled using the parabolic equation. The modelled results agree well with the measurements.

Keywords

BOTTOM LOSS
CROSS-CORRELATION
ELBA
ITSA
LOW REQUENCY
MULTIPATH
PSEUDO-RANDOM NOISE
SHALLOW WATER
SOUND SPEED PROFILE
STRAIT OF FLORIDA
SUMMER

CONTENTS

1. Introduction, 1

2. Measuring method, 2

3. Measurement area, 6

4. Acoustic travel time, 9
   4.1 FLUCTUATION IN TRAVEL TIME, 9
   4.2 AT 15 km RANGE, 9
   4.3 AT 20 km RANGE, 14
   4.4 AT 34 km RANGE, 16
   4.5 SUMMARY, 16

5. Correlation loss, 18
   5.1 COMPUTATION, 18
   5.2 AT 15 km RANGE, 18
   5.3 AT 20 km RANGE, 22
   5.4 AT 34 km RANGE, 22
   5.5 SUMMARY, 22

6. Transmission loss, 26

7. Conclusions, 31

Acknowledgements, 31

References, 32

1. Introduction

To assess the problems that might arise in locating the position of an acoustic pinger at long ranges in shallow water, measurements were made of the spread in acoustic travel time and correlation loss as functions of range, pulse length, and pulse form. Earlier experiments in shallow water south of Elba during different seasons showed that the acoustic travel time between a fixed sound source and receiver up to 38.7 km apart varied only in the order of 25 ms over several hours [1]. In experiments in the Strait of Florida pseudo-random signals were transmitted from a source on the bottom in 22 m of water to a receiver 43 n.mi away [2]; the bottom profile between these locations showed a 400-m-deep shelf between 3 n.mi and 13 n.mi, followed by a comparatively sharp drop to a depth of 800 m. With a downward-refracting sound-speed profile to the bottom, the set of multipath arrivals down to 14 dB below the strongest arrival lasted for 210 ms. However, no significant variations in the travel times of the main signal were reported.

The experiments described in the present paper were therefore designed primarily to investigate the effect of the multipath on the cross-correlation between different transmitted coded signals and their stored replicas. As we were interested in worst-case situations, i.e., many multipaths and interactions with the bottom, we chose an area with a shallow hard bottom as well as a summer condition with a strong downward-refracting sound-speed profile stretching to the bottom in the shallow area. Signals with a centre frequency of 1087.5 Hz and maximum bandwidth of 50 Hz were chosen. This choice was based on restrictions in the available signal-processing equipment and transducers, as well as on a need to use a low frequency for long-range transmissions.

The measurements took place in shallow water north of the Island of Elba in October 1983.

2. Measuring method

Two ships were involved in the measurements. SACLANTCEN T/B MANNING was anchored in 60 m water depth and lowered a transmitter first to 10 m above the sea floor and then to the sea floor itself. SACLANTCEN R/V MARIA PAOLINA G. (MPG) was anchored in about 200 m water depth and deployed a vertical string of hydrophones. The hydrophones were decoupled from the ship and wave motion by an arrangement of a floating swing trellis and a table (15 m long) whose dimensions were such that about 6 m of the tube gave enough lift to suspend the string of hydrophones and ballast (Fig. 1).

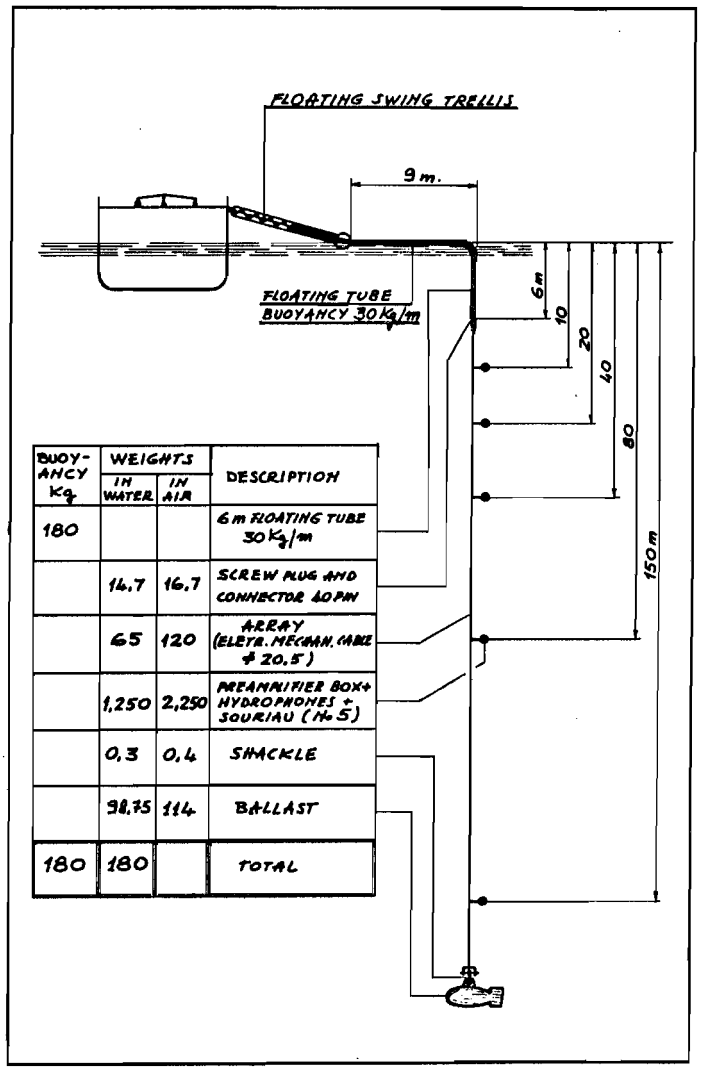

BUOYANCY Kg	WEIGHTS IN WATER	WEIGHTS IN AIR	DESCRIPTION
180			6 m FLOATING TUBE 30 Kg/m
	14.7	16.7	SCREW PLUG AND CONNECTOR 40 PIN
	65	120	ARRAY (ELETR. MECHAN. CABLE Φ 20.5)
	1,250	2,250	PREAMPLIFIER BOX + HYDROPHONES + SOURIAU (N° 5)
	0,3	0,4	SHACKLE
	98,75	114	BALLAST
180	180		TOTAL

Fig. 1. Description of hydrophone array and deployment.

Report no. changed (Mar 2006): SM-191-UU

Both linear FM sweeps and pseudo-random noise (PN) signals were transmitted. Each transmission consisted of a sequence of pulses (see Table 1).

TABLE 1

Transmitted signals

SEQUENCE	SIGNAL
A	2 s linear FM up-sweep 0.5 s blank 4 s linear FM down-sweep 0.5 s blank 8 s linear FM up-sweep
B	4 s linear FM down-sweep 0.5 s blank 16 s linear FM up-sweep
C	2 s PN 25 Hz* 0.5 s blank 4 s PN 25 Hz 0.5 s blank 8 s PN 25 Hz
D	4 s PN 25 Hz 0.5 s blank 16 s PN 25 Hz
E	2 s PN 50 Hz 0.5 s blank 4 s PN 50 Hz 0.5 s blank 8 s PN 50 Hz
F	4 s PN 50 Hz 0.5 s blank 16 s PN 50 Hz

*PN frequencies are the chip repetition rates.

Report no. changed (Mar 2006): SM-191-UU

The measurement system is shown in Fig. 2. All the signal processing was done on board MPG, using the ITSA system [3]. The two ships were in continuous radio contact. A trigger pulse was transmitted via radio from the MPG at 150 s intervals. On being received by MANNING it triggered a transmission of the coded waveform. The trigger pulse was delayed in order to begin the data acquisition just before the acoustic signal arrived at the hydrophones. The maximum uncertainty in the measurement system due to this cause is estimated to be 30 ms.

The ITSA system is limited to analyzing 4 kbytes of data at a time, and this made it necessary to reduce the sampling rate as much as possible. After low-pass filtering and digitizing, the signals from four hydrophones were bandpass-filtered in a programmable digital transversal filter, giving a 50 Hz passband with a 12.5 Hz transition band to -40 dB, centred at 1087.5 Hz, and linear phase response. The signal at the output of the filter was decimated to a sampling rate of 150 Hz, which gave a time window of about 27 s (4096/150) for processing.

The ITSA system was programmed to make a cross-correlation with a stored replica of the transmitted waveform and to compute the correlation loss, i.e., the difference between the observed peak value of the cross-correlation function and the peak value that would be observed if the signal had not been modified by the medium. The -6 dB frequency band of the transducer used as a transmitter stretched from 800 Hz to 4 kHz, so that the influence of the transducer itself on the transmitted waveform was assumed to be negligible. This was also confirmed by the very low correlation loss that was sometimes measured.

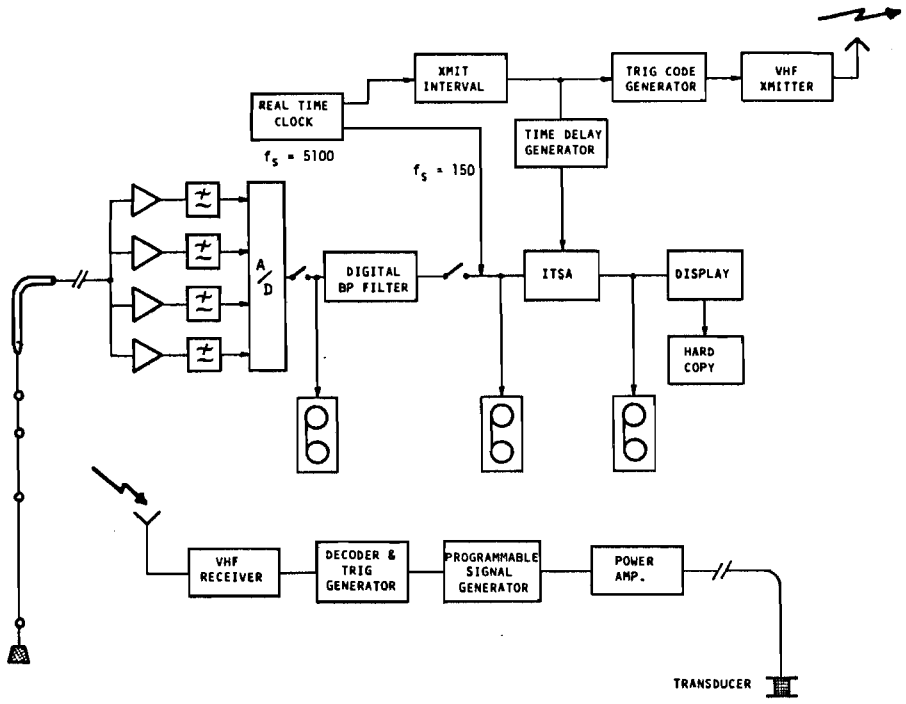

Fig. 2. Acoustic measurement system.

To simulate the narrow-band transducer that would most probably be used in an acoustic pinger, the pseudo-random noise sequence was filtered in a 50 Hz bandpass filter before being fed to the power amplifier.

The replicas for the pseudo-random signals were the actual waveforms generated by a crystal-controlled special-purpose digital signal generator with a 50 Hz bandpass filter on the output. The waveforms were loaded directly into the computer before the sea trial. An attempt was made to first record a series of sequences of pseudo-random signals on an analogue FM tape recorder (type B & K 7003) and then to choose one of the recorded signals of each sequence as a reference and load this in the computer. The result was a correlation loss that varied by several decibels from signal to signal in the same sequence played back from the tape. When the reference was loaded directly from the signal generator a maximum cross-correlation loss of 0.2 dB was observed, even for the longest signals. A similar maximum correlation loss was measured for the FM signals when synthetic replicas generated within the ITSA system were used.

During the tests the following data from each of the four hydrophones were computed in real time:

- Travel time of the largest cross-correlation peak in ms.
- The cross-correlation function in the time window ± 1 s from the peak.
- Acoustic signal power on the hydrophone in dB//1μPa.
- Acoustic noise power on the hydrophone in dB//1μPa.
- Correlation loss in dB
- Propagation loss in dB.

An example of the real-time display of a 16 s FM sweep is shown in Fig. 3. This is taken from the longest range, where a soft lossy bottom reduced the amplitudes and number of multipaths. The peak is the time at which the acquisition system was triggered.

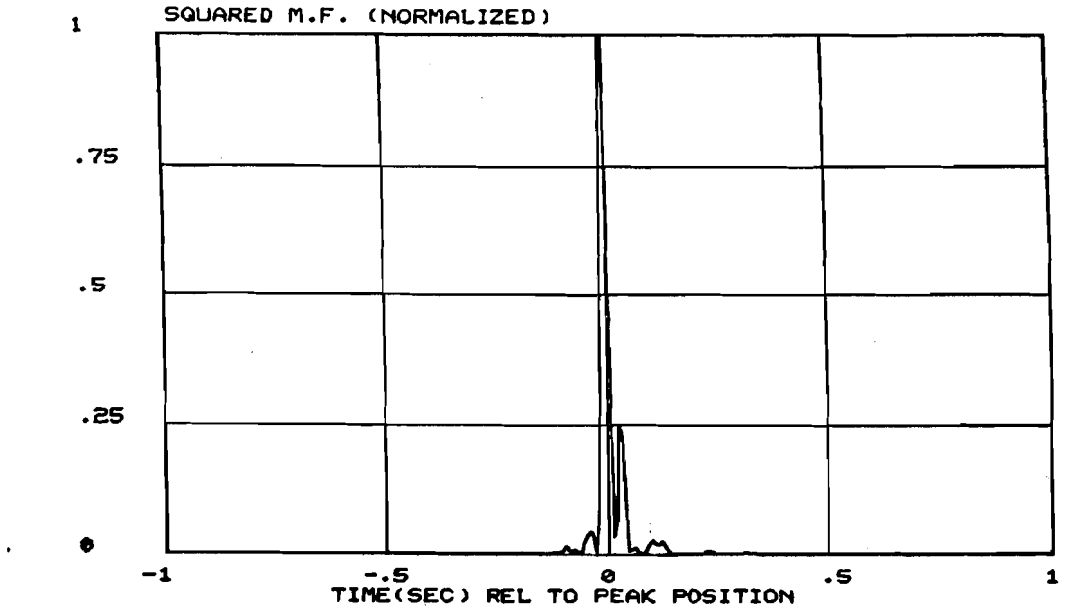

Fig. 3. Real-time display of a 16 s FM sweep.

3. Measurement areas

Figure 4 shows the area north of Elba where the measurements were made. Sediment cores in this area were lacking but cores were available from areas just south of the area of the longest range. The transmitter was sited at positions A, B, and C. The MARIA PAOLINA G. (with receiver) was positioned at D for all measurements. Core 116 from the measurements made by Akal et al, [4] and [5], shows that the upper 90 cm is clay in which porosity decreases from 74% to 50% where it overlies a sand layer (see Fig. 5). Further north, where the measurements over the two shorter ranges took place, detailed sea charts classify the bottom sediment as sand.

The bathymetry for the three ranges are plotted in Fig. 6; the data for the 15 km and 34 km ranges were taken from detailed sea charts; those for the 20 km range were measured. The typical sound-speed profile for both the deep and shallow part of the range is shown in Fig. 7. It changed very little over the two days of experiments and shows a downward-refracting part stretching to the bottom for the shallow section of the transmission path.

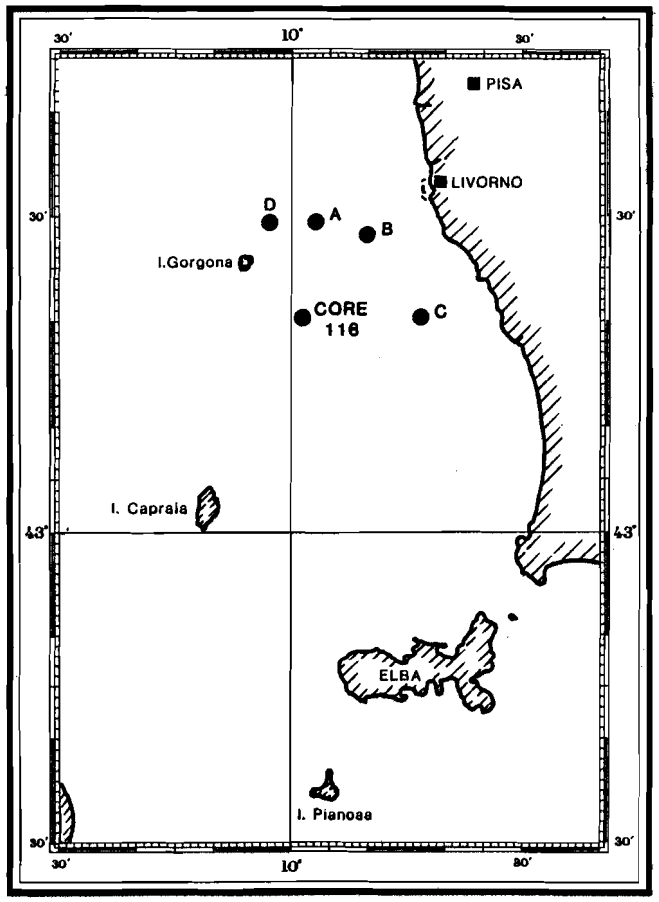

Fig. 4. Area of investigation.

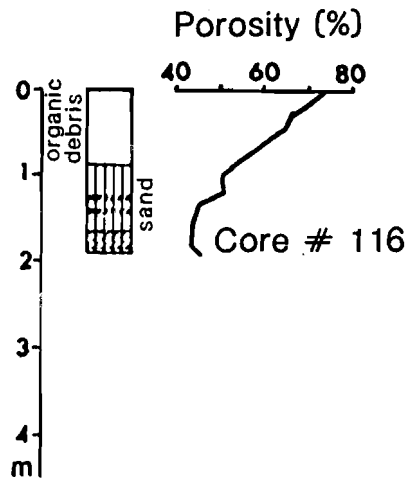

Fig. 5. Porosity and sediment type of the North Elba core.

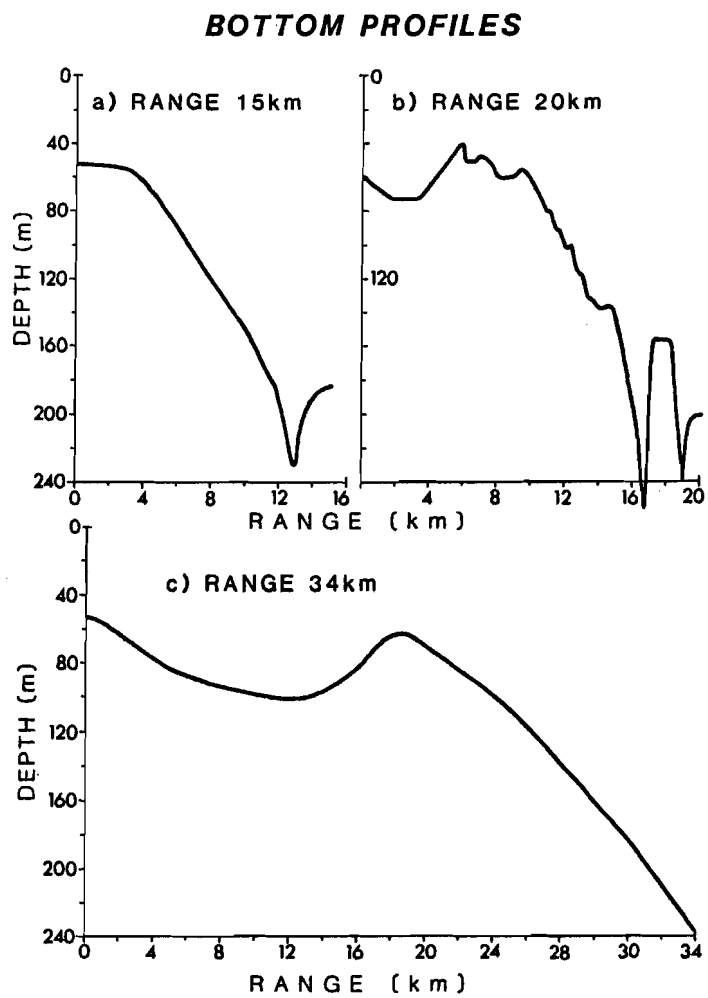

Fig. 6. Bottom profiles along propagation paths.

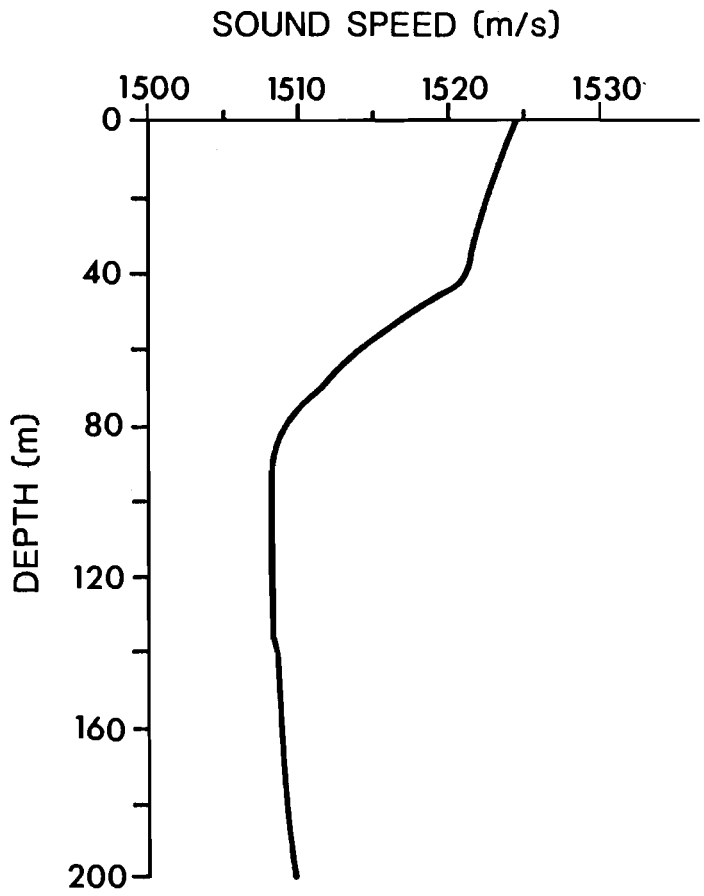

Fig. 7. Typical sound-speed profile of area.

4. Acoustic travel time

4.1 FLUCTUATION IN TRAVEL TIME

To locate the position of an acoustic pinger it is important that the time delay between transmission and reception of the signal (i.e. the acoustic travel time) is predictable. In these experiments the geographical positions of the string of hydrophones and the transmitter was not known accurately enough to measure the difference between expected and measured times of arrival of the sound at the hydrophones. The experiments were thus limited to measuring the fluctuations in the acoustic travel time when transmitting both linear sweep (FM) and pseudo-random (PN) signals.

4.2 AT 15 km RANGE

Figure 8 shows the arrival times of those 16 s signals that gave the highest cross-correlation value on each of the four hydrophones. This was for the shortest range, with a mean travel time between transmission and reception of 9.8 s. During most of the transmissions the transmitter was hanging 10 m above the bottom; however, this does not explain the fluctuations, because the transmission over 20 km range (see Sect. 4.3) shows the same pattern when the transmitter was lying on the bottom for long periods. The fluctuations are more likely to come from the large number of multipaths generated by the downward-refracting sound-speed profile and the hard bottom. Figure 8 indicates that we generally have the same variation in arrival times at all the hydrophones; however, the fluctuations at the deepest hydrophone (at 80 m) are less than those at the others. Especially for transmission number 7, we see a big difference in arrival times between the hydrophones at 40 m and 80 m.

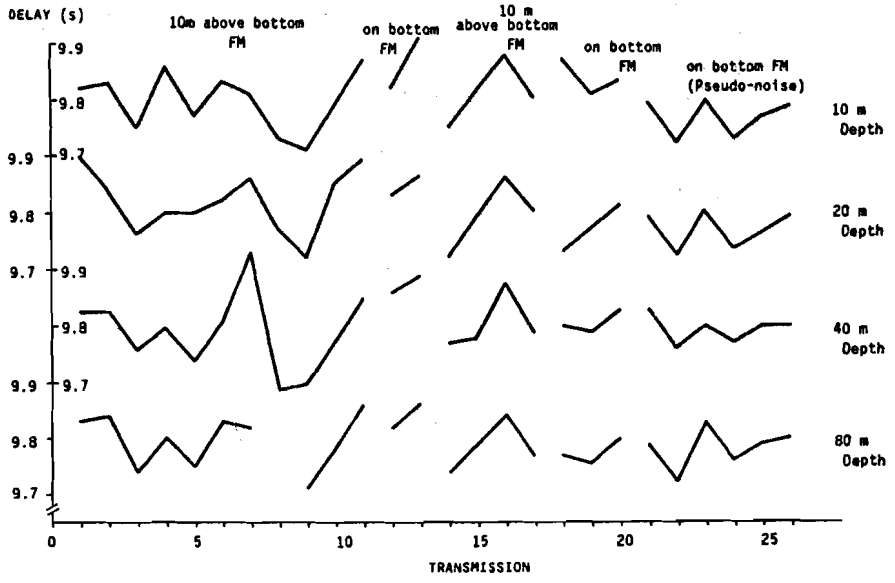

Fig. 8. Arrival 16 s signals with highest cross-section value on each of 4 hydrophones for 26 transmissions.

The reasons for this difference become clear when we look at the squared magnitude of the cross-correlation function for these two hydrophones in Fig. 9a, b. The multipath problem is more severe for the hydrophone at 40 m depth, with several arrivals competing to give the highest cross-correlation value. The two cross-correlation functions in Fig. 9a, b are individually scaled to give a maximum cross-correlation value of unity; for the transmission shown here, the peak in Fig. 9b is 11 dB higher than that in Fig. 9a. Apparently the spread of the signal due to multipath is about the same for the hydrophones whether at 40 m or 80 m.

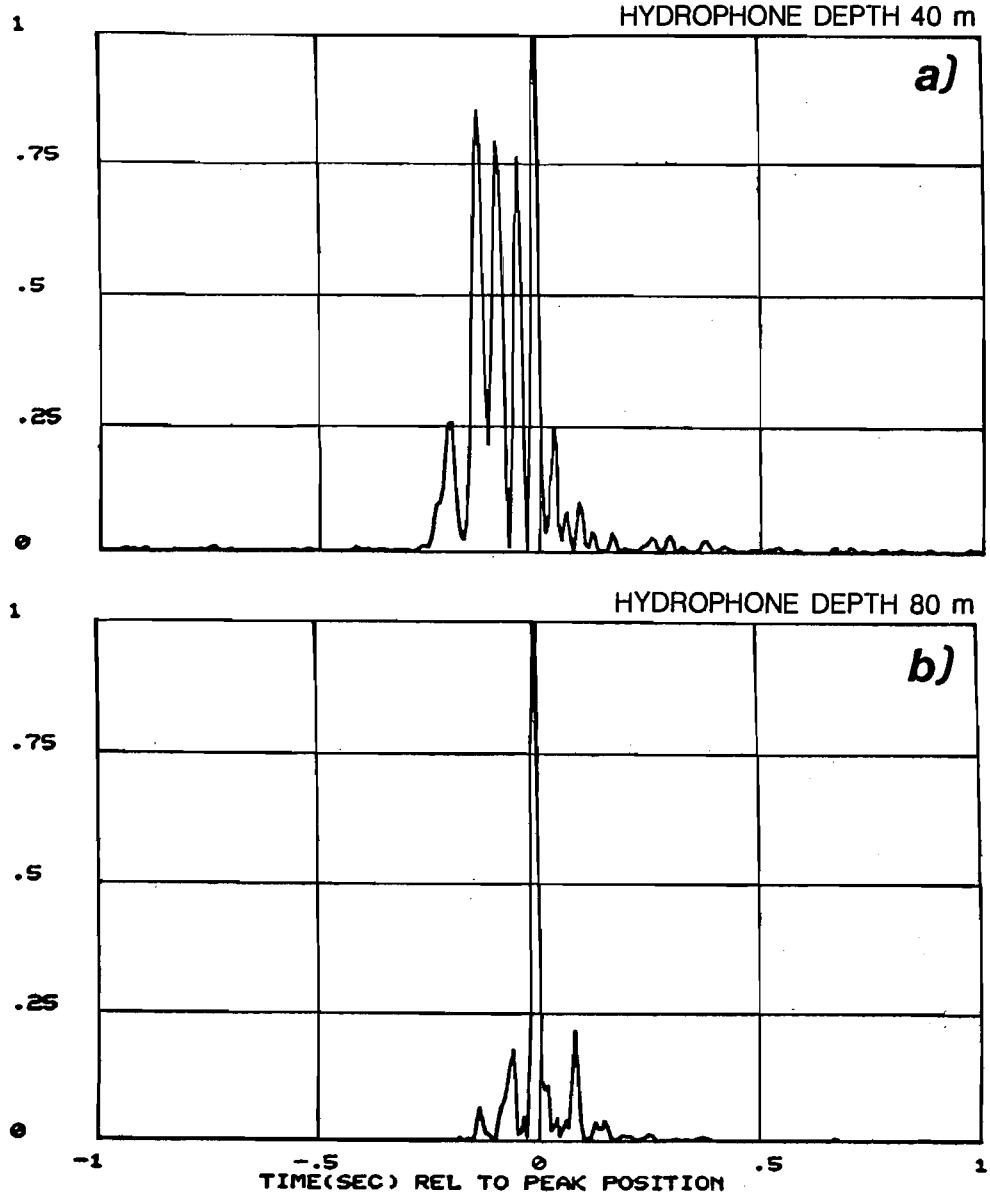

Fig. 9. Squared magnitude of the cross-correlation function for transmission number 7 received at the hydrophone at (a) 40 m depth, (b) 80 m depth.

Figure 10 shows the different arrivals due to multipath for each 16 s transmission. A spread of up to 300 ms can be found in the data from the 40-m-deep hydrophone, Fig. 10a. Apparently the multipath structure is fairly stationary, while the peak in the cross-correlation function jumps between the different possible acoustic paths from transmitter to hydrophone as small changes in the environment change the constructive and destructive interference pattern at the site of the hydrophone array.

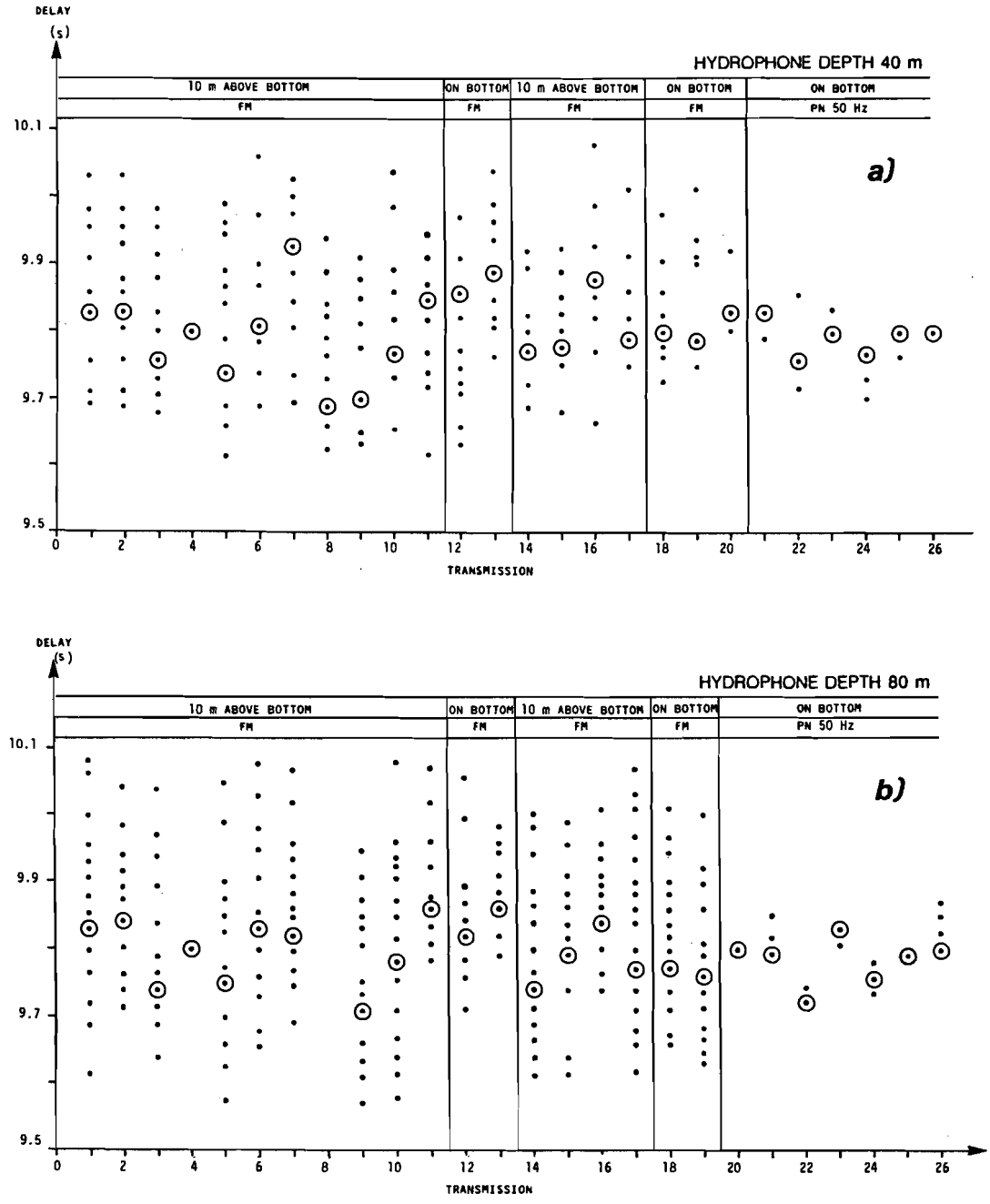

Fig. 10. Multipath arrival 16 s transmissions (circled points represent strongest arrivals): (a) hydrophone at 40 m, (b) hydrophone at 80 m.

Figure 11 presents ray traces for the 15 km range, using the GRASS model [6]. The traces show that most of the acoustic energy that reaches the hydrophones at 40 and 80 m depths derives from multiple refections with the surface and bottom. A small change in exit angle changes the ray path drastically, indicating that the interference pattern created by the different rays is very sensitive to small changes in the sound-speed profile.

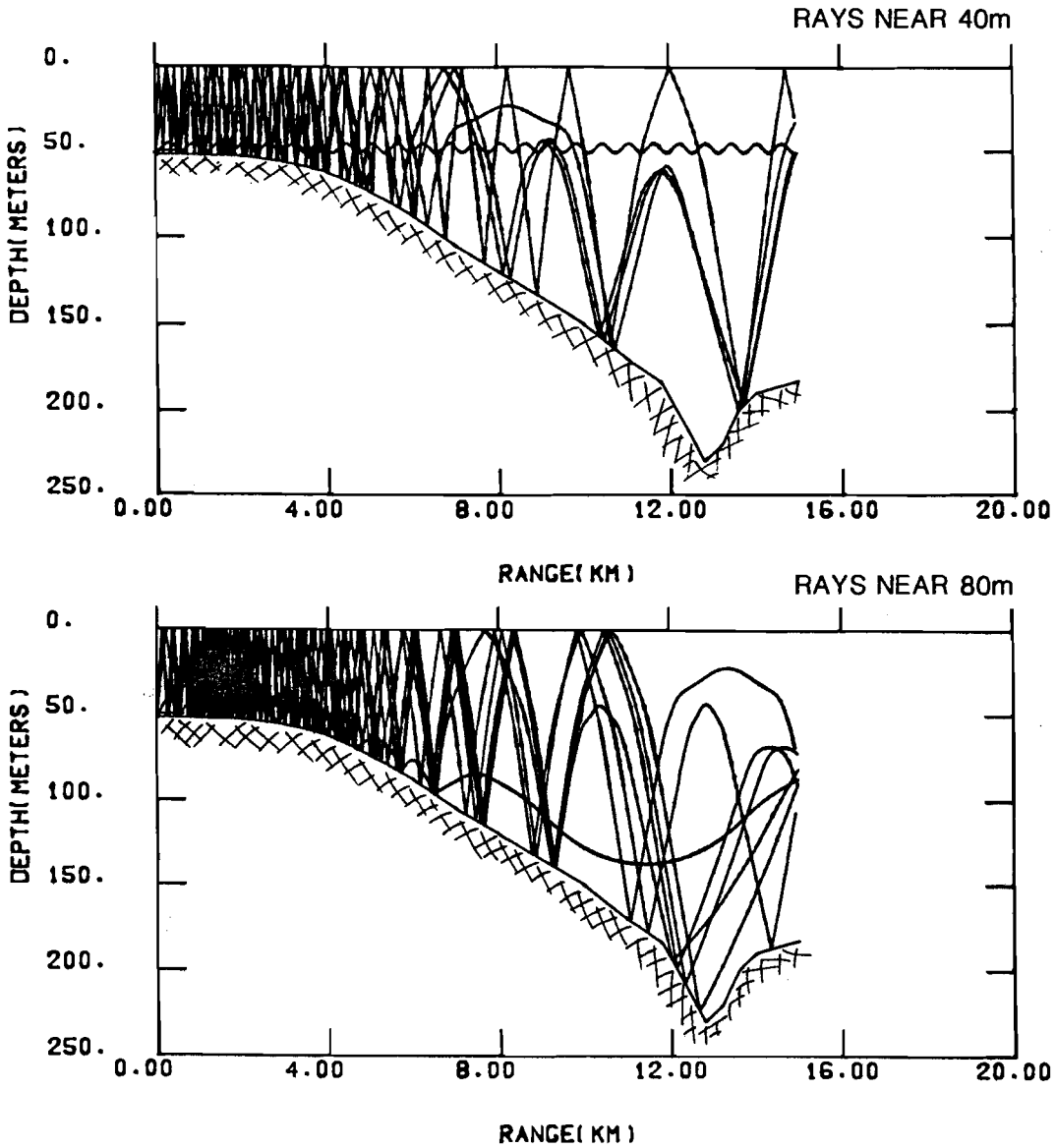

Fig. 11. Ray arrives at 40 and 80 m depths.

If the signal-to-noise ratio is small, only the highest peaks are detected, and the "stationarity" of the multipath structure disappears. This is seen on Fig. 12, which shows only those arrivals that exceed a fixed threshold set at 3 dB below the weakest peak in the cross-correlation functions computed for a run (a series of transmission with 150 s intervals). A system to locate the position of an acoustic sound source should therefore not use the peak in the cross-correlation function to estimate the acoustic travel time between sound source and receiver. The appealing thought, based on Fig. 10, of using the mean arrival time of a cluster of multipath arrivals for the estimate proves, according to Fig. 12, not to be much better than using the peak of the cross-correlation function. The best estimate of the acoustic travel time apparently will derive from use of the first arrival that exceeds a threshold set at a fixed distance above the noise level. Coincidentally, this results in the simplest receiver. By using the first arrival above the fixed threshold of Fig. 12, the peak-to-peak fluctuation reduces from 240 ms to 135 ms on the 40-m-deep hydrophone and from 150 ms to 130 ms on the 80-m-deep hydrophone.

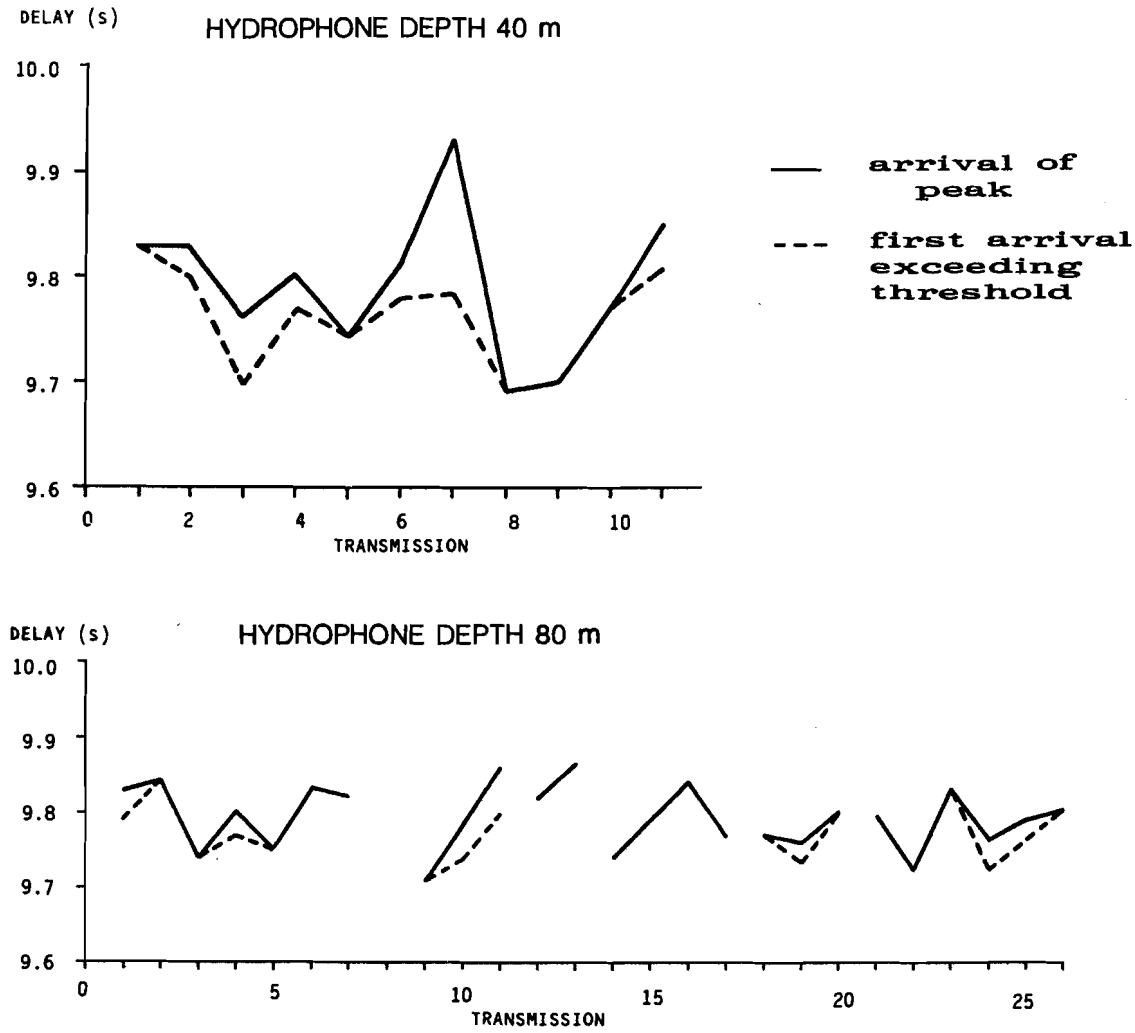

Fig. 12. Arrival time of signals that exceed the threshold (3 dB below the lowest cross-correlation peak measured in each run). Transmitted signal 16 s linear FM sweeps and 50 Hz PN sequence.

4.3 AT 20 km RANGE

The same types of measurement were carried out over a distance of 20 km, the main difference being that the transmission was across a 30 m high seamount, as shown in Fig. 6b. Figure 13 shows the acoustic travel times measured to the peak of the cross-correlation function (peak delay) and to the time when the cross-correlation function first exceeded a threshold 6 dB below the peak level (detection delay). The actual travel time is shown for the 16 s signal, while the 8 s, 4 s and 2 s signals are shifted by 0.3, 0.6 and 0.9 s respectively. The results shown for the hydrophones at 40, 80 and 160 m depth are very similar to those in Fig. 8. There seems to be little difference in fluctuations for the different signal lengths and waveforms. The deepest hydrophone has the least spread in travel

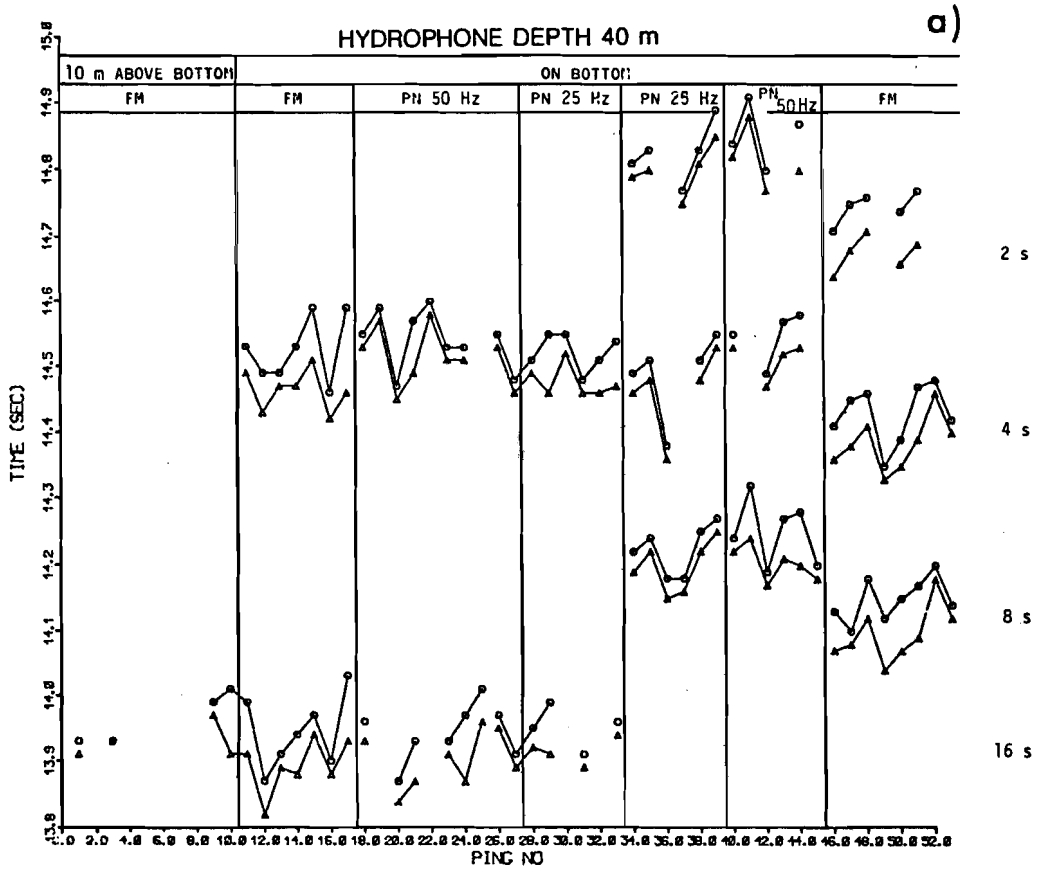

Fig. 13. Travel time for transmissions over 20 km range. Signals were transmitted every 150 s. Actual travel time is shown for each 16 s signal; the other signals are shifted up by 0.3, 0.6, and 0.9 s respectively.

o peak delay

Δ detection delay

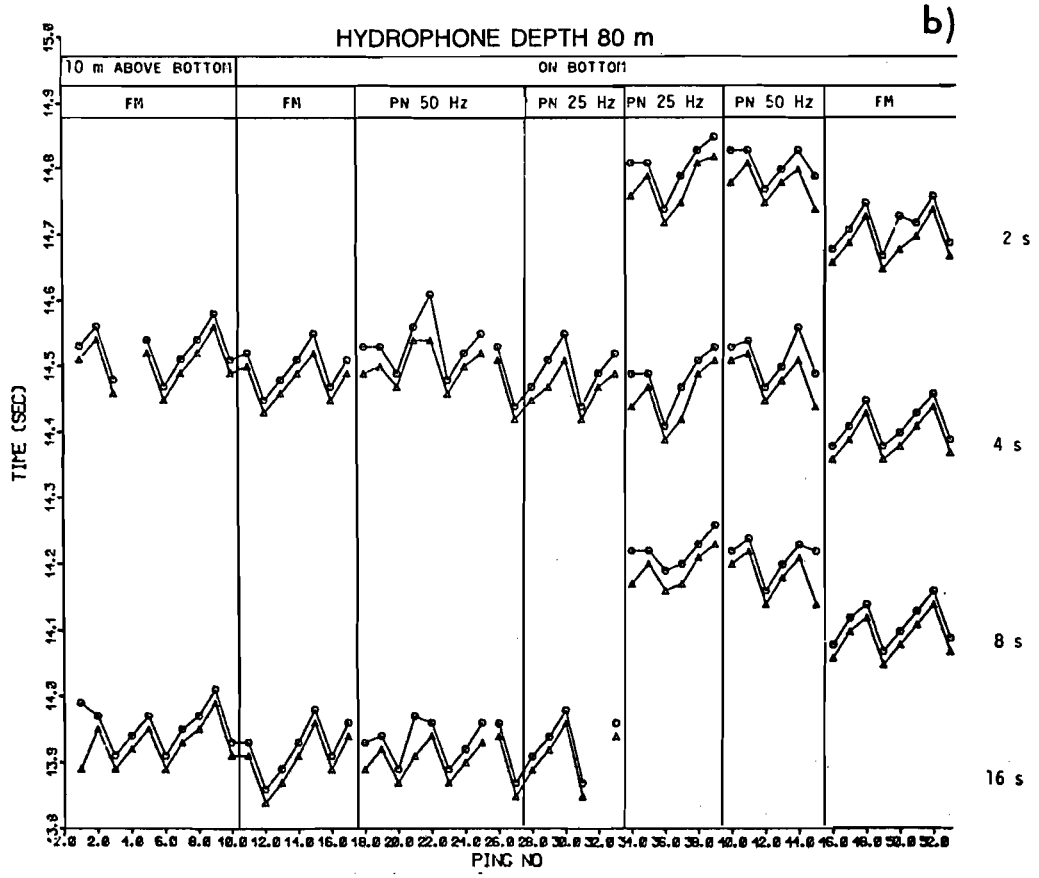

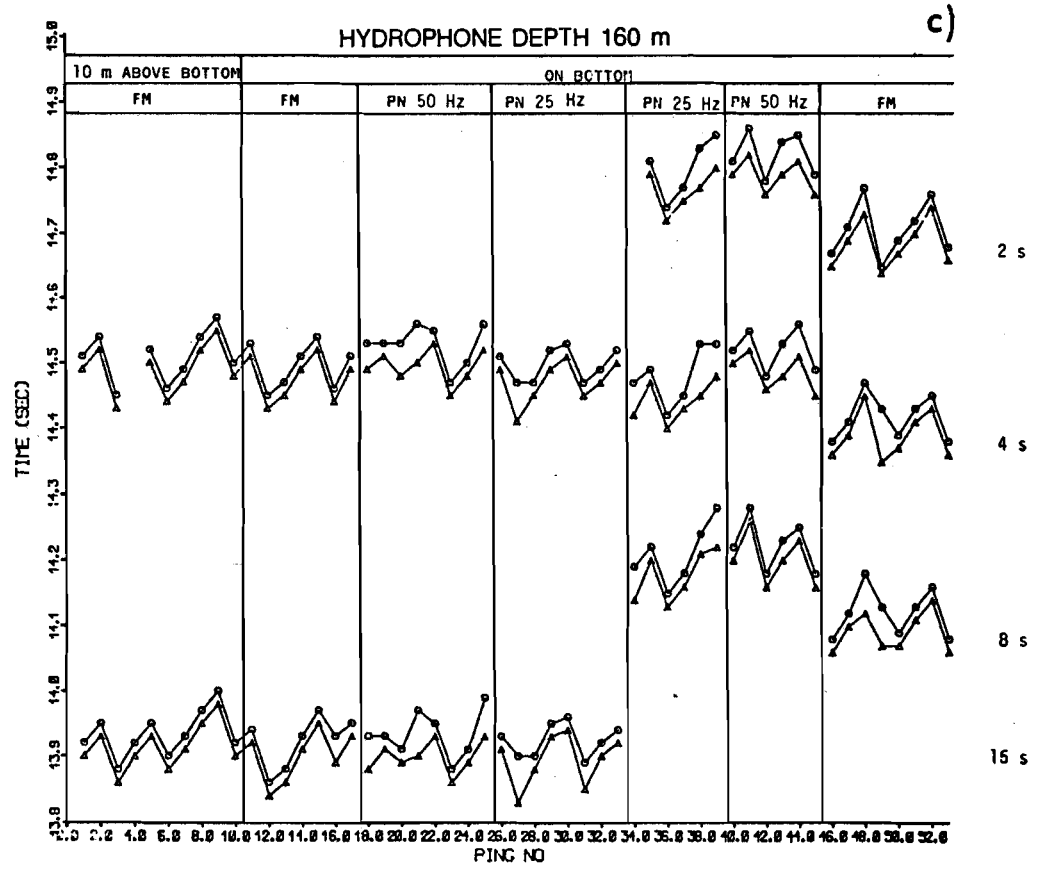

Fig. 13. Continued.

times, a peak-to-peak spread of about 130 ms as before. Between transmissions 45 and 46 there was a interval of about 45 min when the transmitter was lifted off the bottom and the MANNING allowed to swing on its anchor, resulting in a different transmitter location from transmission 46 onwards.

4.4 AT 34 km RANGE

The final transmission experiments were over a range of 34 km. There the bottom structure had a layer of porous clay or mud above the sand layer. Lacking core data from this area we can only assume that the bottom is lossy. The results of the measurements are shown in Fig. 14, using the same definition for the peak and detection delay as in Sect. 4.3. A 16 s signal followed by a 4 s signal was transmitted every 150 s, with a 17.5 min interval between transmissions 2 and 3 and a 35 min interval between transmissions 8 and 9.

The fluctuations in travel time have almost disappeared when one looks at the first arrival 6 dB below the peak of the cross-correlation function (detection delay). However, the peak still fluctuates about 100 ms on all the hydrophones except for the one at 160 m, which shows a very stable travel time. These measurements correspond more closely with those made south of Elba by Sevaldsen [1], who reported fluctuations of the order of 40 ms when two strong arrivals were present, but of only about 5 ms when one strong arrival was observed.

4.5 SUMMARY

The results indicate that even with the severe multipath propagation observed in this area the peak-to-peak fluctuation in the travel time is about 130 ms, equivalent to about a 200 m peak-to-peak fluctuation in the range measurement. At long ranges (34 km) where the bottom near the transmitter is softer, the fluctuation was reduced to the uncertainties in the measurement system of about 30 ms, which is equivalent to a range fluctuation of about 45 m.

The best receiver structure seems to be a matched filter followed by a detector with a fixed threshold set at a given distance above the ambient noise.

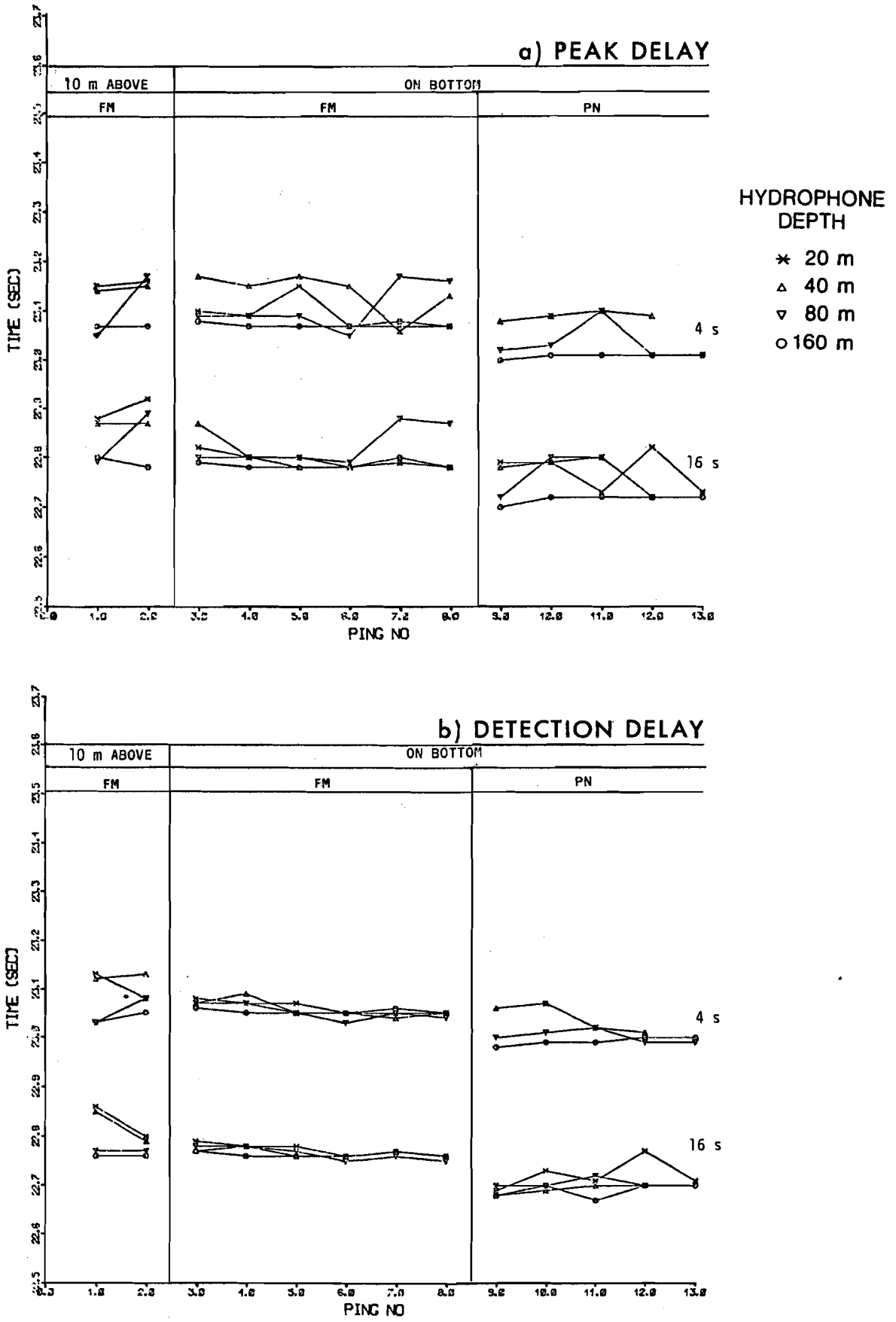

Fig. 14. Travel time for 13 transmissions over 34 km range. One transmission every 150 s in each run. Actual travel time is shown for the 16 s signal; the 4 s signal has been shifted up by 0.6 s.

Report no. changed (Mar 2006): SM-191-UU

5. Correlation loss

5.1 COMPUTATION

The correlation loss was computed as the difference between the achieved processing gain and the theoretical gain observed when signal and reference signal were perfectly matched and no noise was present. The formula used was:

$$L = 10 \log \frac{\sum[(r_i + n_{1i}) - n_{2i}] \cdot S_i^*}{\sqrt{[(\sum(r_i + n_{1i})^2 - \sum n_{2i}^2] \cdot \sum S^* S_i}}$$

where

(r_i+n_{1i})= the received signal samples corrupted by noise. Note that r_i and n_{1i} cannot be separated.

n_{2i} = noise samples measured when no signal was present. We assume that the noise is stationary, so that the energy of (n_{1i}) is the same as that of n_{2i}.

S_i = reference signal samples.

It is seen that a positive signal-to-noise ratio at the input of the receiver is needed for (r_i+n_i) to be a measure of the signal. This made it difficult to obtain reliable results for the shallow hydrophones because of their proximity to the MPG, which is noisy even in "silent" conditions.

5.2 AT 15 km RANGE

The correlation losses for 16 s and 4 s signals transmitted in sequence over the 15 km range are shown in Fig. 15. Only the results from signals that gave a positive signal-to-noise ratio at the input are shown. Generally, those transmissions that experienced a severe multipath propagation in which several paths had equivalent significant amplitudes are the ones that show high correlation loss, since the transmitted energy has been spread out over several paths. An example is transmission number 7 of the 16 s FM sweep received at the 40- and 80-m-deep hydrophones. The two cross-correlation functions are shown in Fig. 9. Both show a similar spread of multipath in time, but the multipath signals received by the 80 m hydrophone are weaker, resulting in a correlation loss that is 5.2 dB less for this transmission than that measured on the 40 m hydrophone (see Fig. 15c and d).

At 10 m depth the correlation loss for the 16 s FM sweep is consistently greater than for the 4 s FM sweep during the first five transmissions. Again this is due to the energy being spread over more high-amplitude multipath signals for the 16 s signal than for the 4 s signal. Figure 16 compares the two signals, 16 s and 4 s, transmitted in the second sequence.

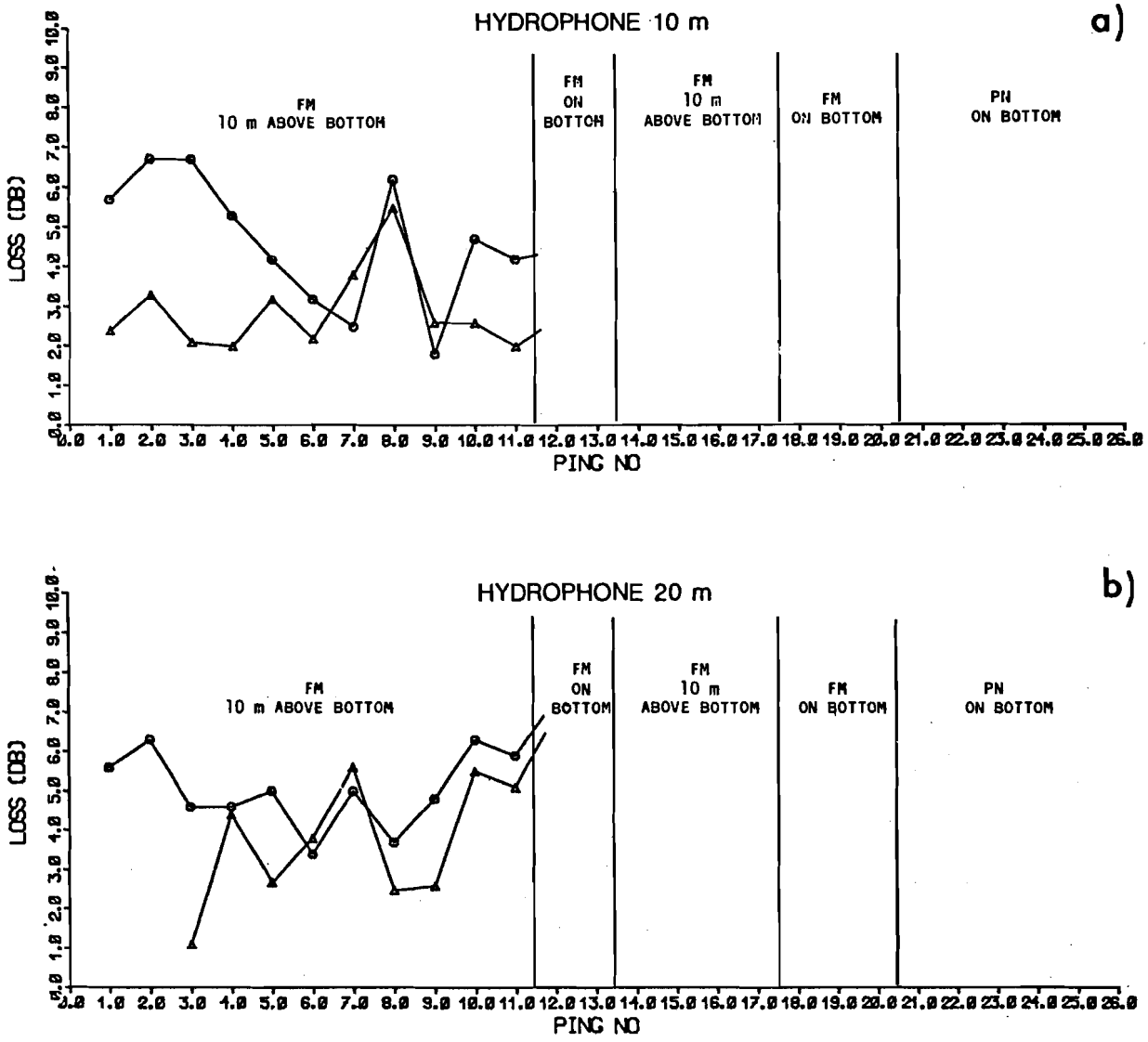

Fig. 15. Correlation losses at range of 15 km for 4 s and 16 s signals.

△ 4 s
○ 16 s
lin FM

✳ 4 s
▽ 16 s
50 Hz PN

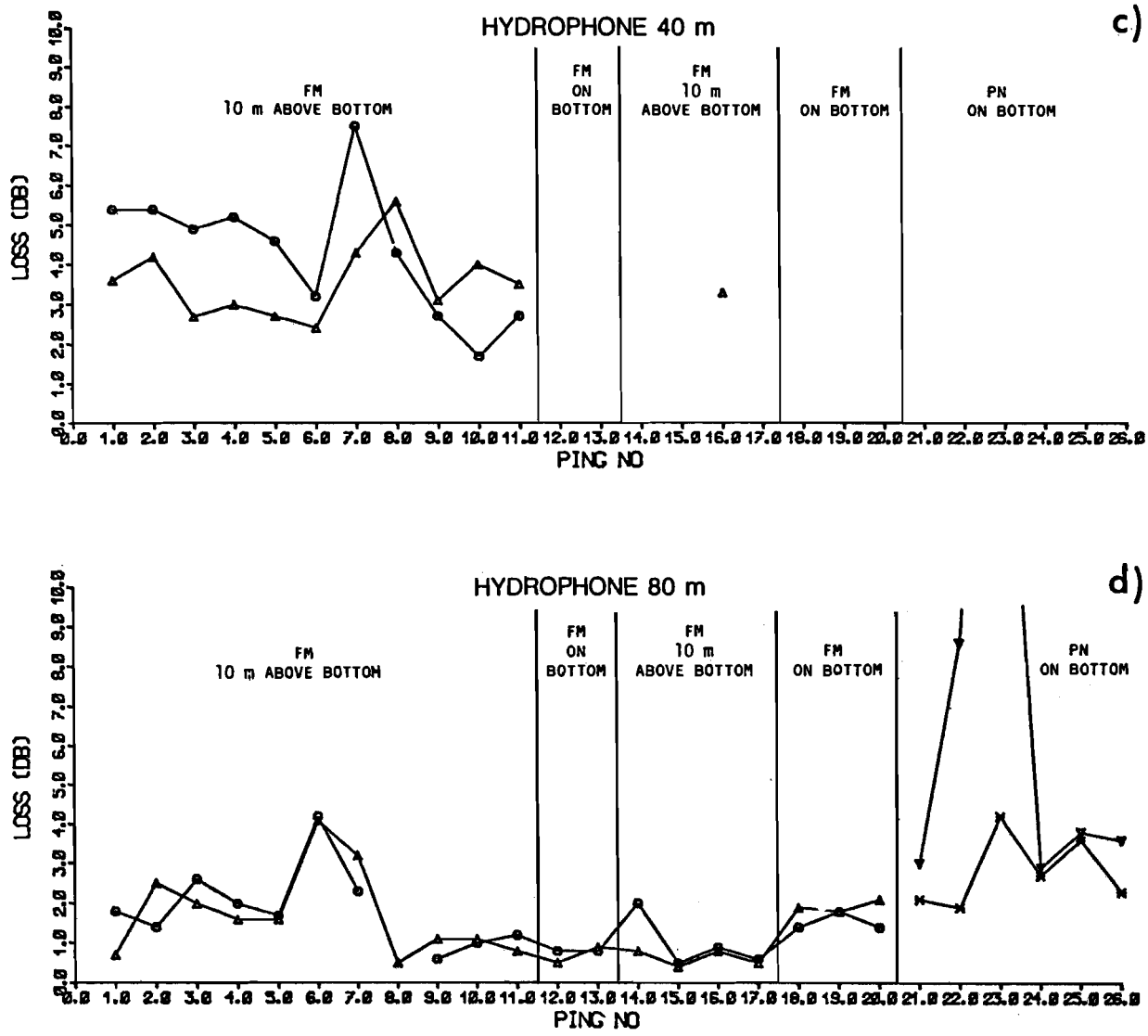

Fig. 15. Continued.

△ 4 s
○ 16 s
lin FM

✳ 4 s
▽ 16 s
50 Hz PN

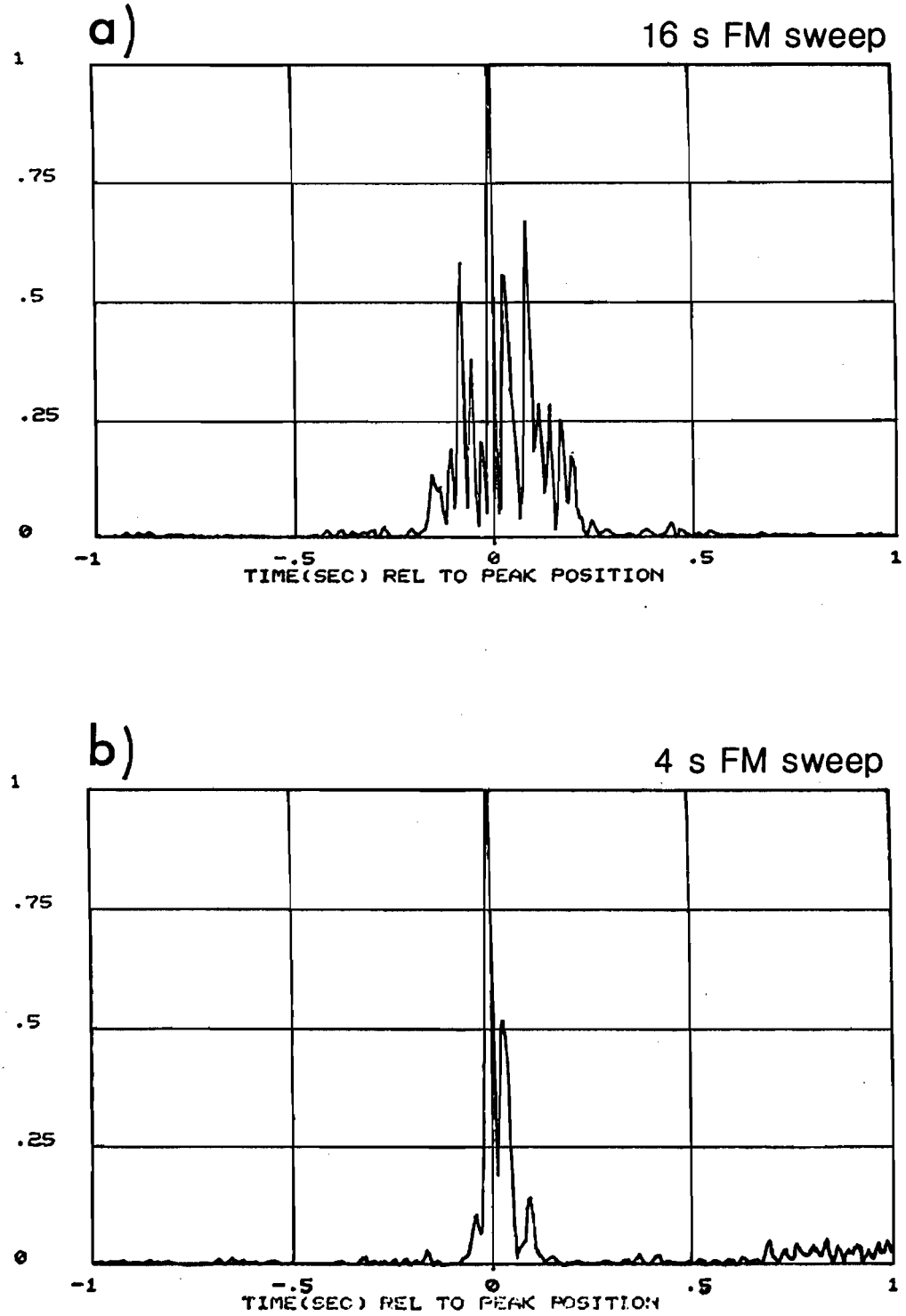

Fig. 16. Cross-correlation function of the 16 s and 4 s signals of transmission no. 2 received by the hydrophone at 10 m depth.

After the first eleven transmissions, data are available only for the 80-m deep hydrophone because a step-up transformer to the transducer malfunctioned, reducing the output level by 8 dB; the received signal level thereby became less than the noise level before processing. The signal on the deepest hydrophone, in this case 80 m, shows a much more stable correlation loss than the other. There are only small differences between the 4-s- and 16-s-long signals, except for the pseudo-random noise signal (PN) which indicates higher correlation loss than for FM signals with the same time/bandwidth product. This is especially seen for the 16 s pseudo-random noise signal, as expected from Sevaldsen's measurements south of Elba [1]. He found that, in summer conditions and at our ranges, the frequency spreading due to the medium was of the order of 1 Hz when the transmitter was on or near the bottom.

5.3 AT 20 km RANGE

For the 20 km range only the correlation loss from the hydrophones at 80 and 160 m are shown, Fig. 17. Again it is seen that the long pseudo-random noise signal has a much higher variability in the correlation loss than the fm and short pseudo-random noise signals. There is little difference between the fast chip rate of 50 Hz and the lower one of 25 Hz; this indicates that the correlation loss is due more to frequency spreading of the medium than to time spreading. The results must however be taken with a bit of caution as there is the possibility that the vertical string of hydrophones was slowly drifting; thereby introducing doppler shifts that would degrade the pseudo-random noise signals much more than the FM sweep. The 16 s pseudo-random noise signal would not correlate with the replica if the received frequency was shifted 1/16 Hz (63 mHz); however the 4 s signal can tolerate a shift of about 250 mHz. The differences between the 2, 4, 8 and 16 s FM sweeps are small, indicating that FM sweeps even longer than 16 s can be used without increasing the correlation loss.

5.4 AT 34 km RANGE

Only at the lowest, 160 m deep, hydrophone did the transmissions over 34 km give a consistent signal-to-noise ratio above zero before processing; this was due to the lower noise level at that depth. Again the correlation loss for the FM signals, Fig. 18, is much more consistent from transmission to transmission than for the pseudo-random noise signals. This run shows far fewer strong multipaths than the previous runs; consequently the transmitted energy is concentrated more in these few strong arrivals and the correlation loss is less than that found for the shorter ranges. The travel time fluctuation has also virtually disappeared on the deepest hydrophone (see Fig. 14a).

5.5 SUMMARY

The means and the sample standard deviations of the correlation losses for all signals of the same type transmitted at each range are shown in Fig. 19. As noted before, increasing the FM signal length to 16 s apparently doesn't increase the correlation loss. However, the pseudo-random noise signal shows a strong increase in correlation loss with increasing pulse length.

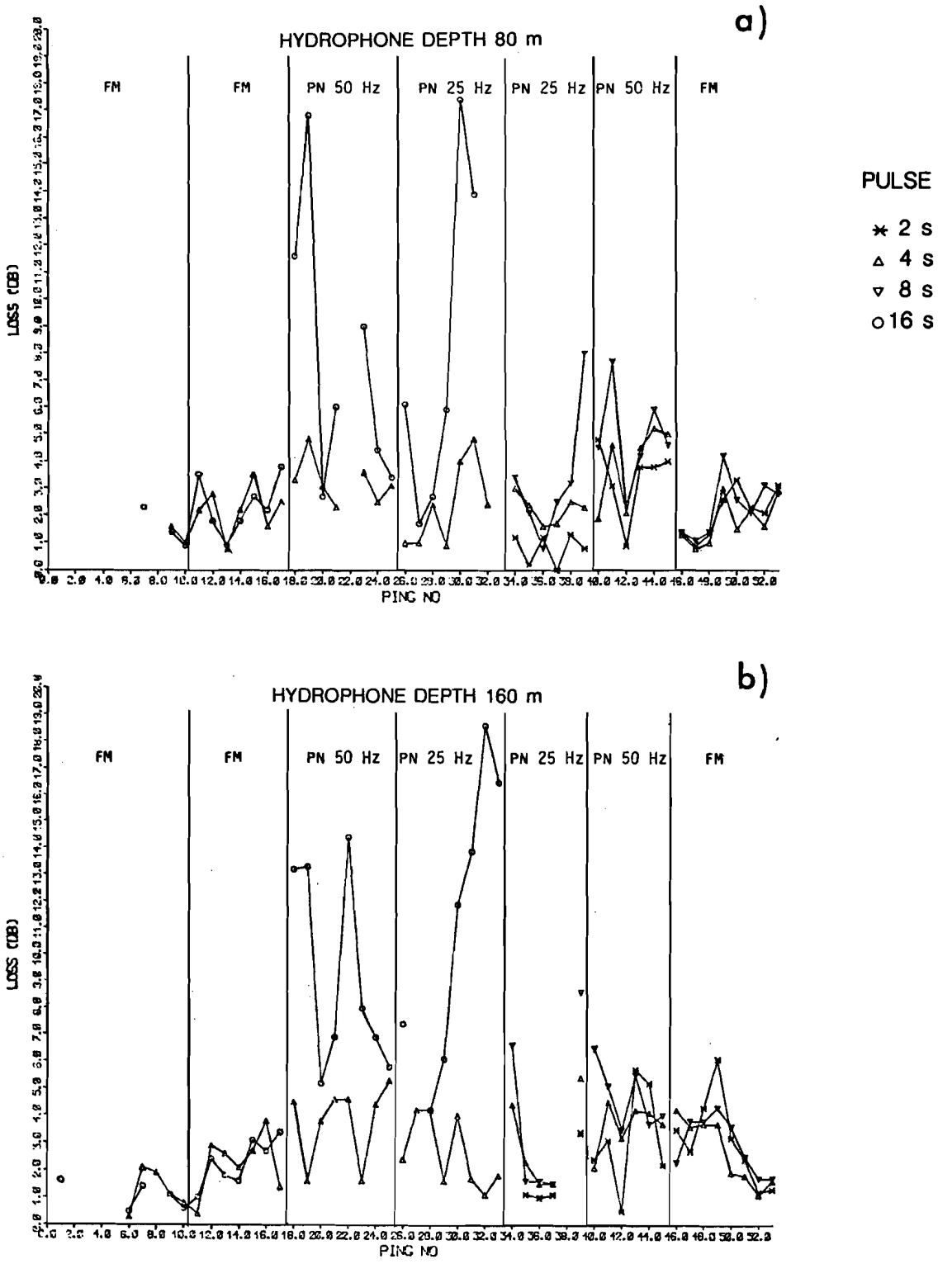

Fig. 17. Correlation loss for 20 km range.

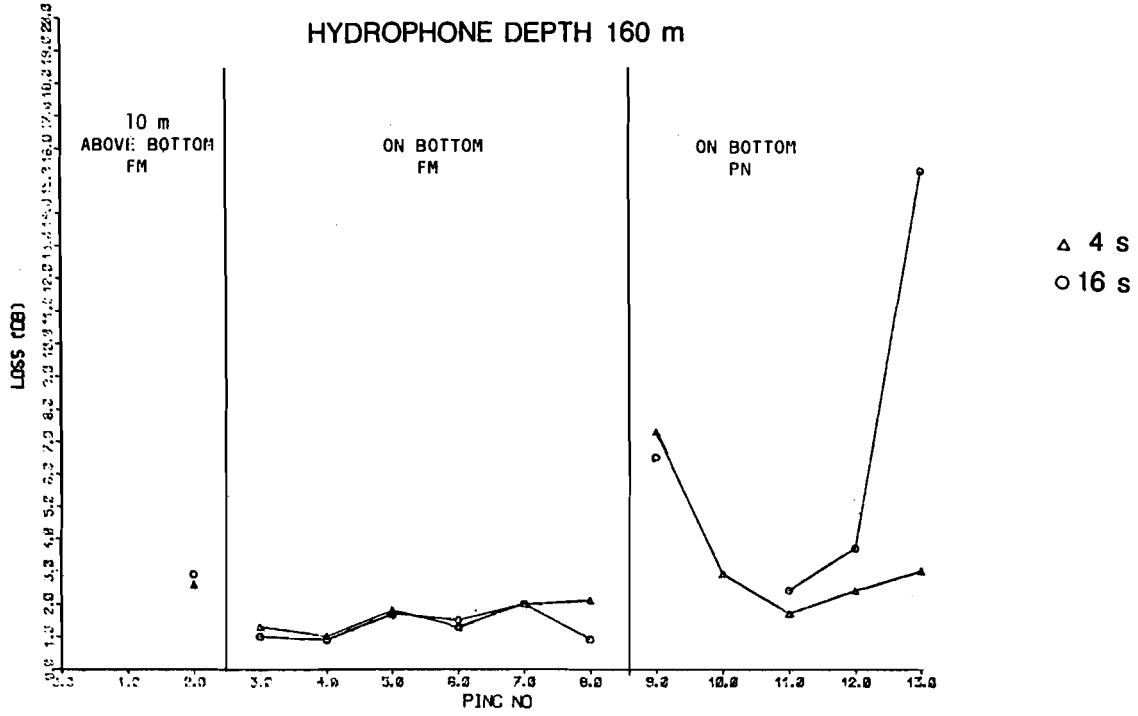

Fig. 18. Correlation loss for 34 km range.

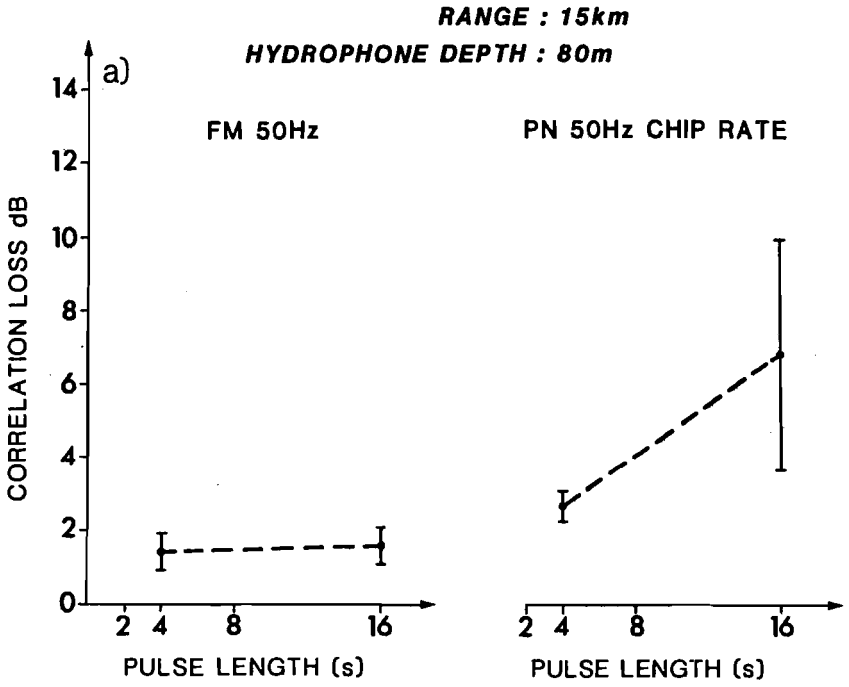

Fig. 19. Mean and sample standard deviation of all signals of each type transmitted at the different ranges.

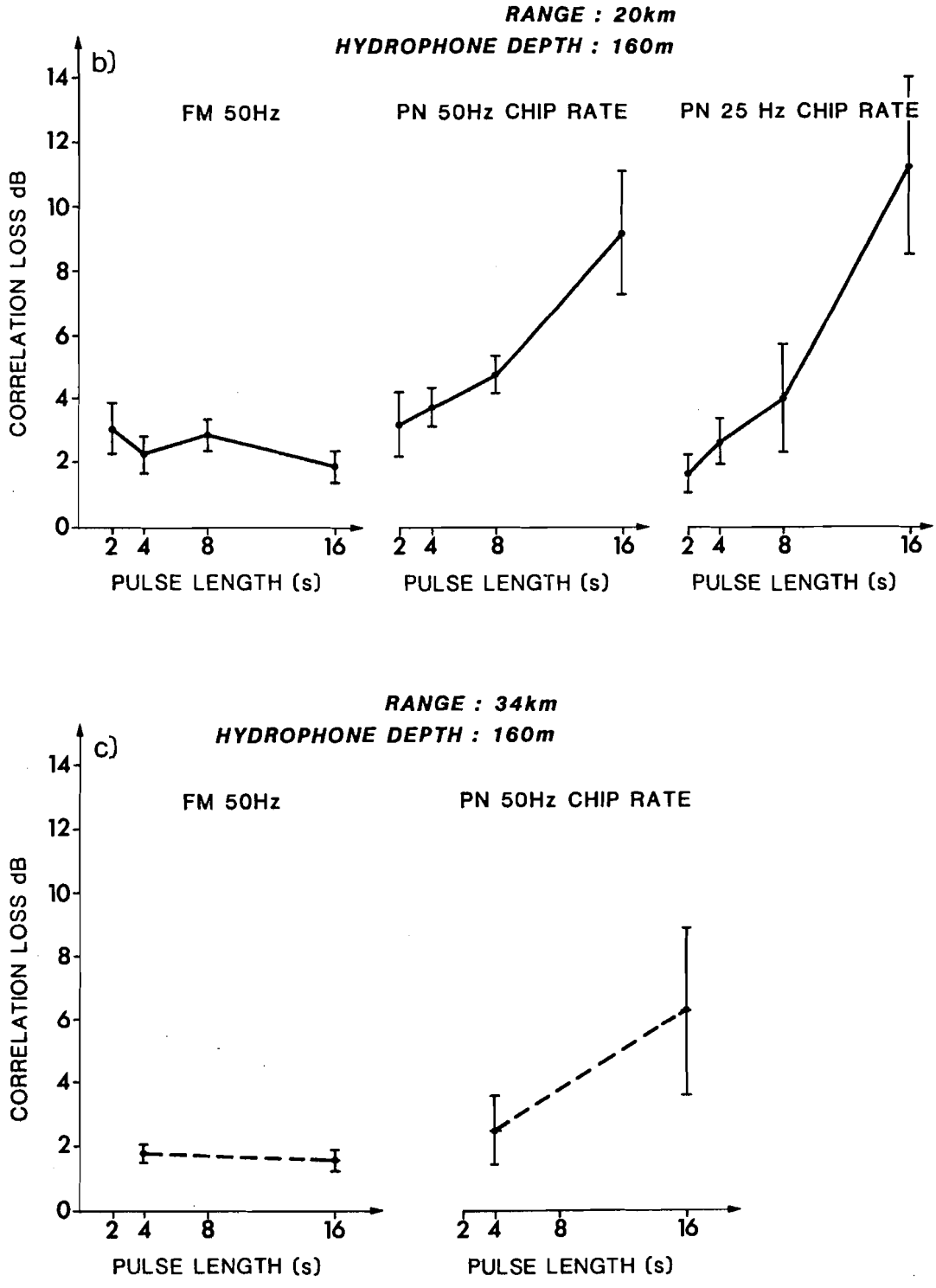

Fig. 19. Continued.

6. Transmission loss

The transmission loss could be measured only with a positive signal-to-noise ratio at the hydrophones. Because the noise level on the shallower hydrophones was generally higher than on the deep ones, we could measure the transmission loss only at four depths (Fig. 20) during the first eleven transmissions when the step-up transformer was working. The three shallow hydrophones, all in the mixed layer, show a higher propagation loss than that of the 80 m deep hydrophone in the weak sound channel (see Fig. 7). The fluctuations are within 5 dB and do not correlate with the rapid fluctuations in the correlation loss.

During the transmissions over 20 km range two hydrophones in the sound channel showed the same trend in transmission loss (Fig. 20b) between 0942 and 1342 local time. The loss for the longest range (34 km) is virtually the same as for the 20 km range, as shown in Fig. 20c. Only the deepest hydrophone had high enough signal-to-noise ratio at the input to give a continuous plot.

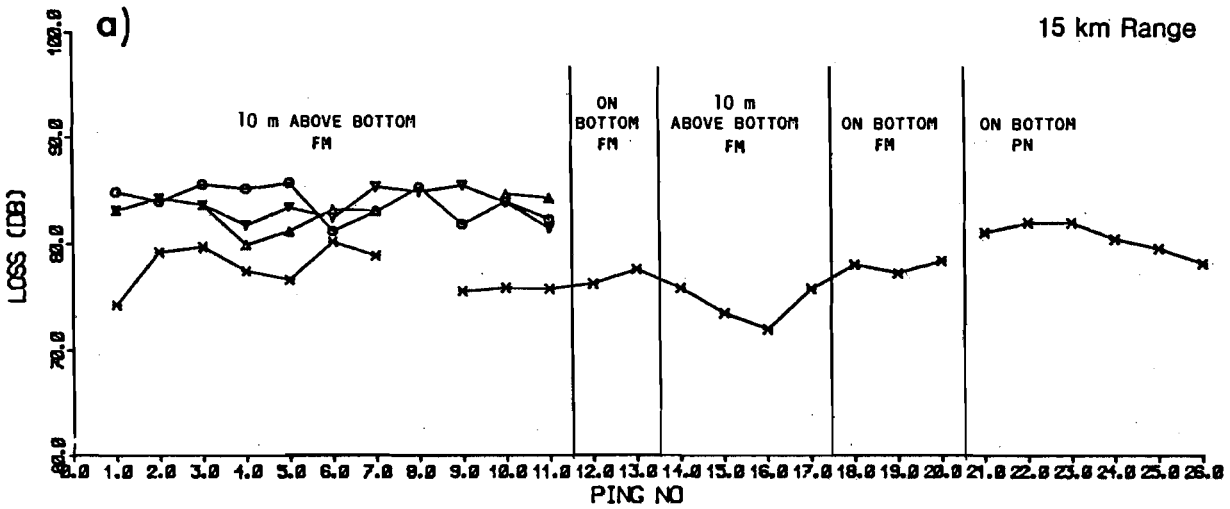

Fig. 20. Propagation loss.

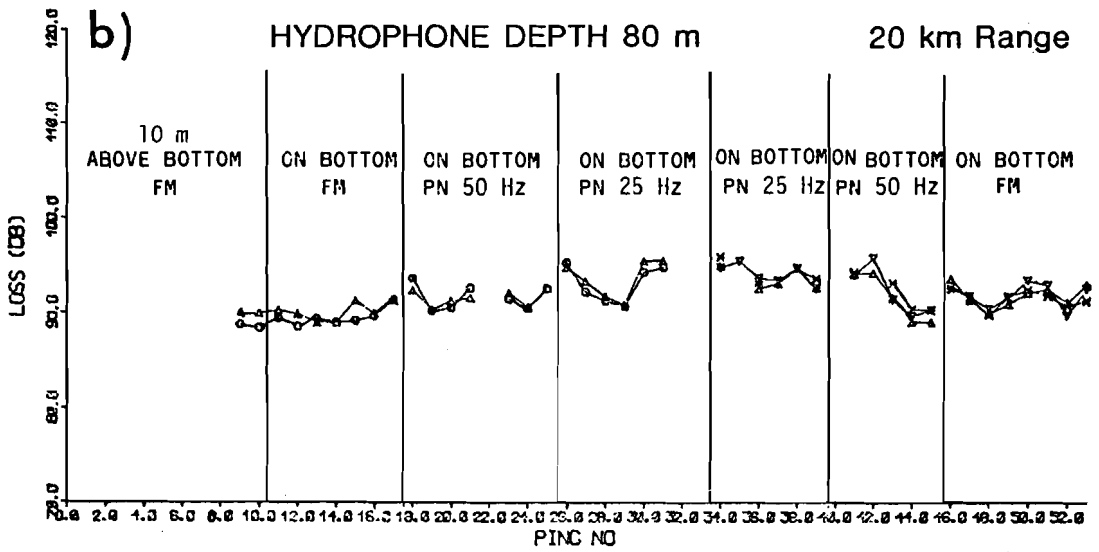

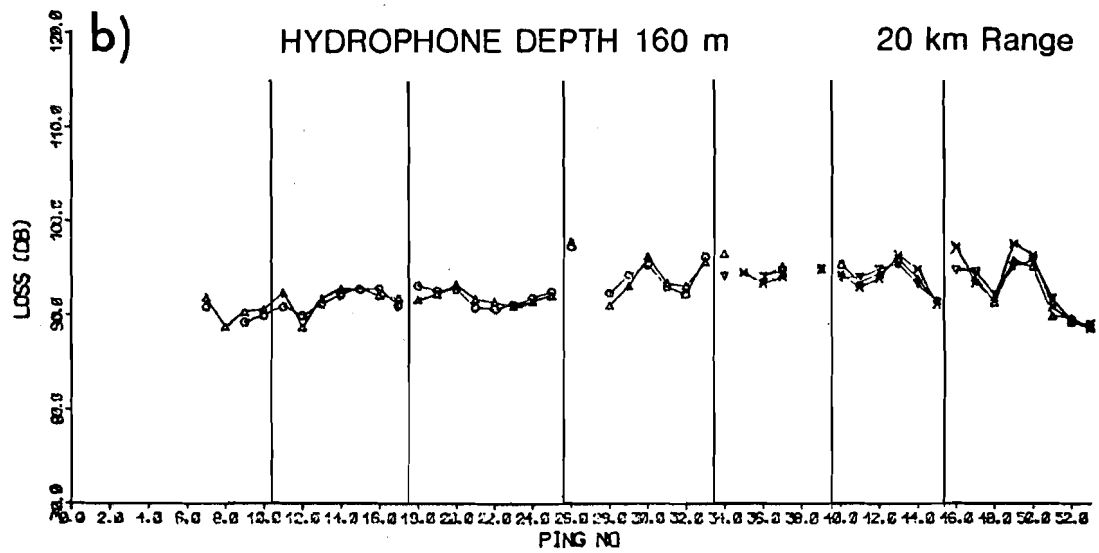

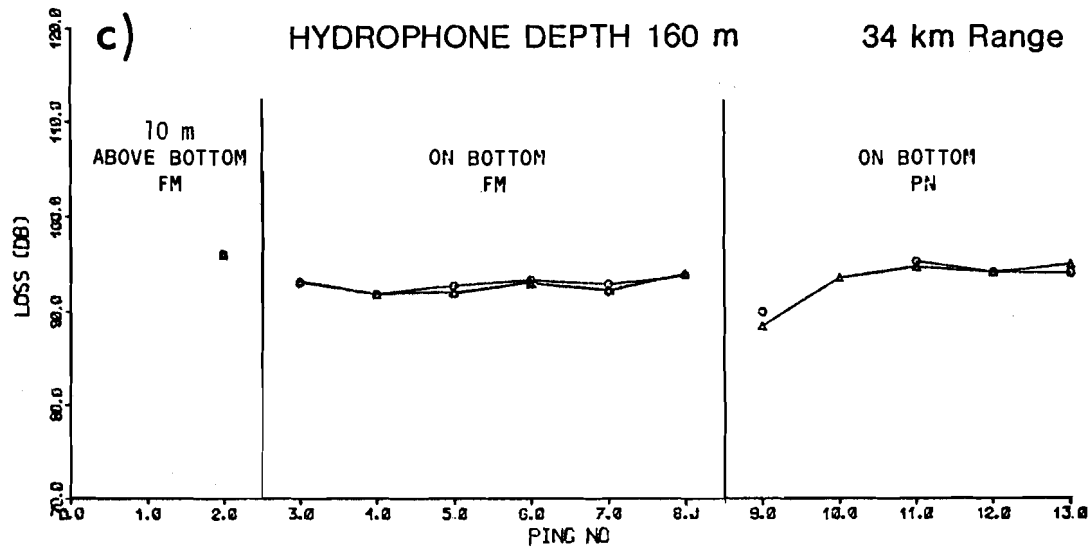

Fig. 20. Continued.

The transmission loss for the 20 km range was computed using the parabolic equation model [7]. The modelled bottom contour is shown in Fig. 21 and the modelled transmission loss to the different hydrophones is shown in Fig. 22. Because the parabolic equation model cannot simulate a source on the bottom, the source and receiver positions had to be interchanged. The model was run four times, each time with the model's source positioned where we had a hydrophone and always with the model's receiver at 60 m, the depth of our source.

As the 60-m-deep modelled receiver is moved away from the source, the transmission loss increases by about the same amount for all modelled source depths. A substantial increase in transmission loss is encountered when the modelled receiver "goes into the bottom" at about 11 km from the modelled source. However, when the modelled receiver "comes out of the bottom" on the other side of the hill, the transmission loss decreases dramatically and we find about 10 dB difference between the modelled sources at 20 and 40 m depth and those at 80 and 160 m depth. The reason for the reduction after we have passed the hill is the strong downward-refracting sound-speed profile. The increase in transmission loss for shallow source depths is also due to the same sound-speed profile, which gives steeper rays that experience more bottom bounces before they pass the hill.

The measured transmission loss is between 90 to 95 dB for the two deepest hydrophones, while the modelled transmission loss is between 87 and 90 dB. The transmission loss at the 20-m- and 40-m-deep hydrophones could not be measured because the signal level before processing did not exceed the noise level.

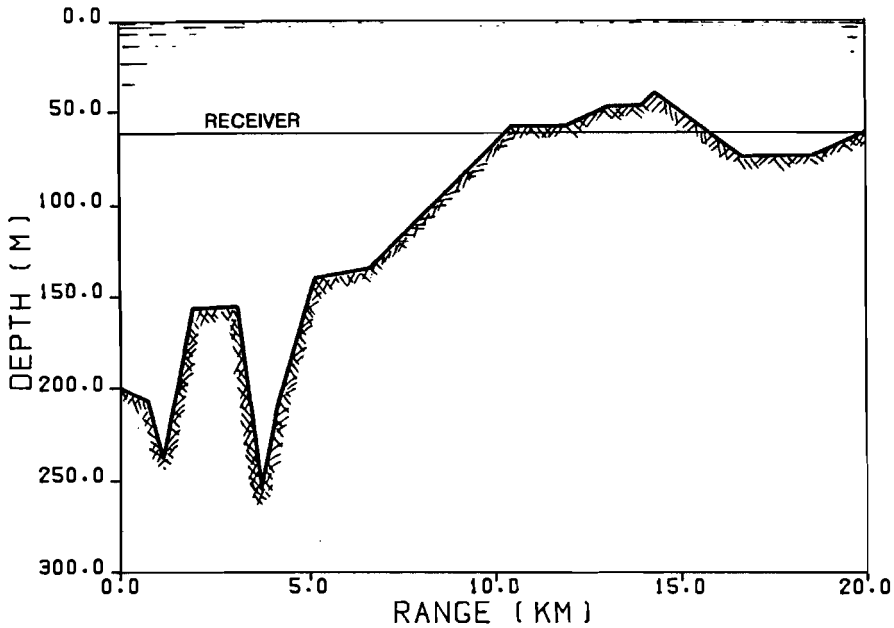

Fig. 21. Modelled bottom contour.

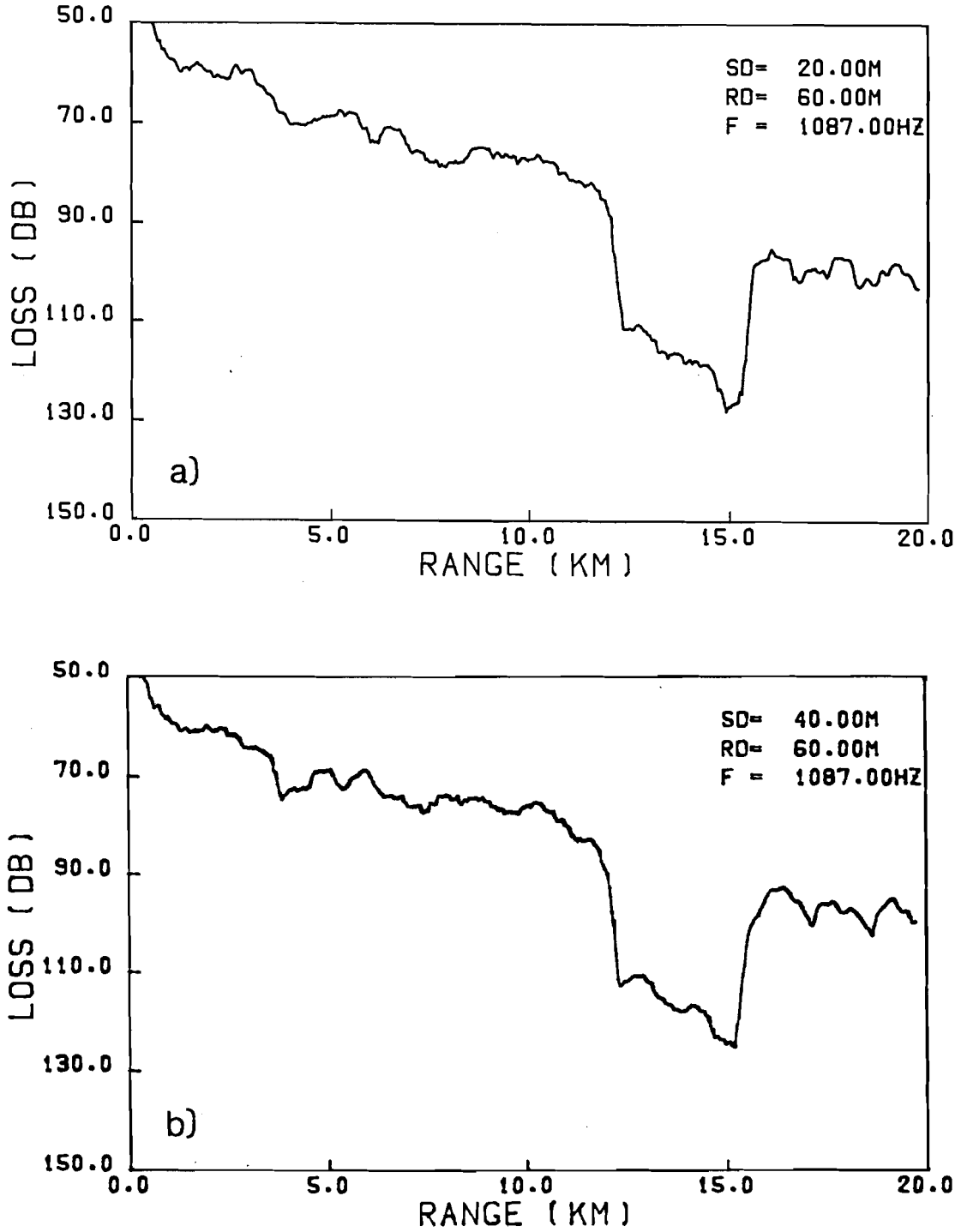

Fig. 22. Modelled transmission loss as a function of source/receiver distance for the 20 km run, using the parabolic equation model.

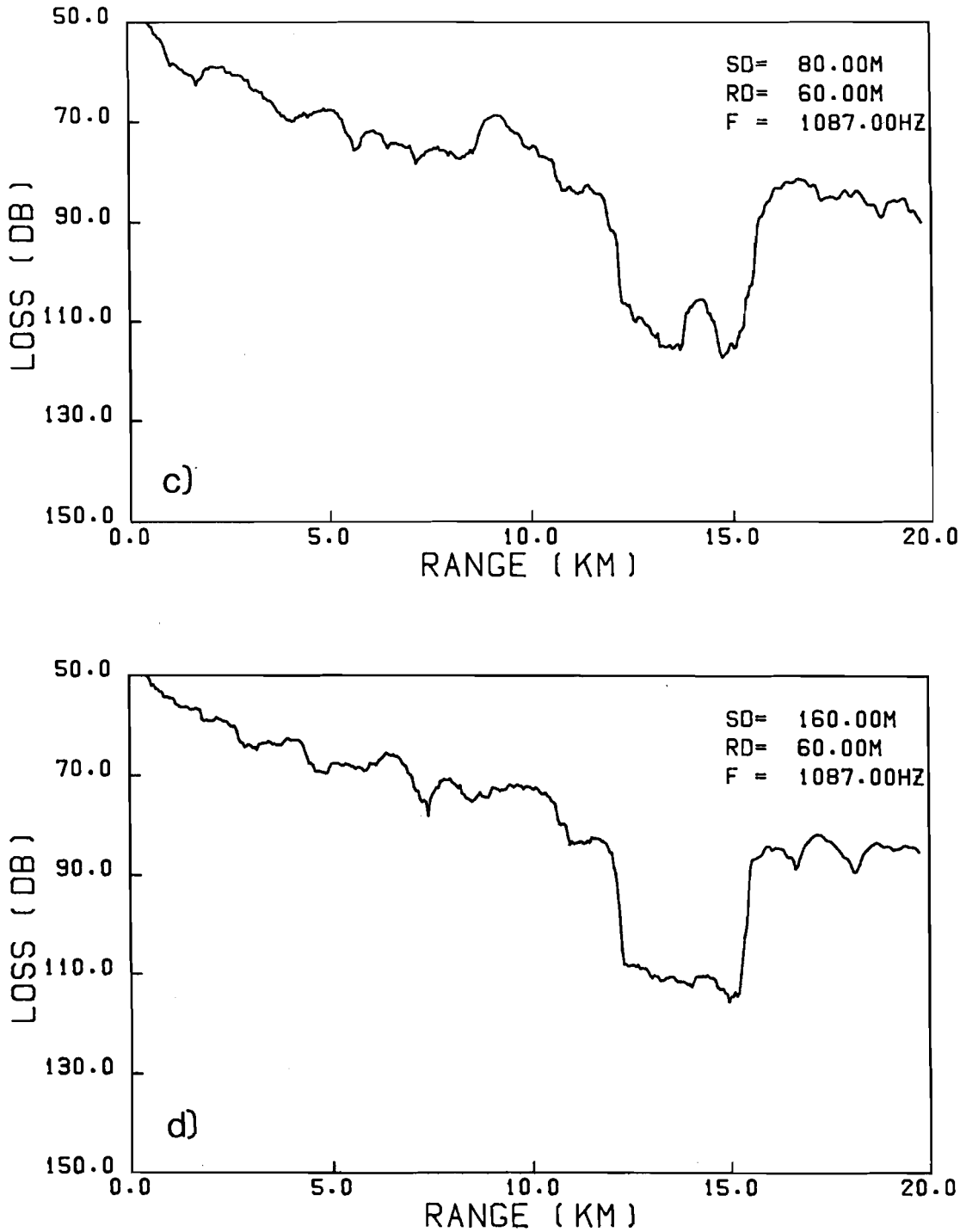

Fig. 22. Continued.

7. Conclusions

The measurements were carried out in a condition that created a strong multipath propagation for the two shorter ranges of 15 and 20 km. The longest range (over 34 km) has a softer, more lossy bottom structure near the transmitter, which almost eliminated the very wide time-spread of the multipath structure. Even in the strong multipath structure the FM sweep signals were not degraded severely. No increase in correlation loss was observed between signal lengths of from 2 to 16 s. The pseudo-random noise signal, however, showed a strong increase in the correlation loss with increasing pulse lengths, almost to the point that the increase in correlation loss would eat up the theoretical increase in processing gain. These results must be taken with some caution because the string of hydrophones was not attached to the bottom; a small drift would increase the correlation loss of the pseudo-random noise signal considerably, but not that of the FM sweep.

The best receiver for detecting the time of arrival of the transmitted signal seems to be a matched filter followed by a threshold detector that compares the output of the matched filter with a threshold set to a fixed level above the noise. In this case it seems that the fluctuations in acoustic travel time can be kept within 135 ms even when the low-level multipath is spread out over almost 400 ms.

Acknowledgements

The contributions of the following SACLANTCEN members to this Memorandum are appreciated.

Experimental Systems Group

E. Bovio — Programming the ITSA systems
E. Capriulo — Preparing computer plots
M. Cassola — Running the GRASS program

Environmental Modelling Group

F. Jensen — Propagation-loss modelling with the parabolic-equation model.

References

[1] SEVALDSEN, E. Variability of acoustic transmissions in a shallow water area, SACLANTCEN SR-46. La Spezia, Italy, SACLANT ASW Research Centre, 1981. [AD A 103 278]

[2] STEINBERG, J.C. and BIRDSALL, T.G. Underwater sound propagation in the Straits of Florida. Journal of the Acoustical Society of America, 39, 1966: 301-315.

[3] SACLANTCEN Real-Time Systems Department. ITSA Manual. La Spezia, Italy, 1977.

[4] AKAL, T. Bathymetry and bottom structure of zones near the Island of Elba used for acoustical trials in shallow water, SACLANTCEN TM-162. La Spezia, Italy, SACLANT ASW Research Centre, 1970. [AD 879 590]

[5] AKAL, T., GEHIN, C., MATTEUCCI, B. and TONARELLI, B. Measured and computed physical properties of sediment cores; Island of Elba zone, SACLANTCEN M-82. La Spezia, Italy, SACLANT ASW Research Centre, 1972.

[6] CORNYN, J.J. GRASS: a digital-computer ray-tracing and transmission-loss-prediction system, volume 1, NRL Report 7621. Washington, D.C., Naval Research Laboratory, 1973.

[7] JENSEN, F.B. and MARTINELLI, M.G. The SACLANTCEN parabolic equation model (PAREQ), VAX/FPS version. La Spezia, Italy, SACLANT ASW Research Centre, 1984.

Report no. changed (Mar 2006): SM-191-UU

INITIAL DISTRIBUTION

MINISTRIES OF DEFENCE	Copies
JSPHQ Belgium	2
DND Canada	10
CHOD Denmark	8
MOD France	8
MOD Germany	15
MOD Greece	11
MOD Italy	10
MOD Netherlands	12
CHOD Norway	10
MOD Portugal	2
MOD Spain	2
MOD Turkey	5
MOD U.K.	20
SECDEF U.S.	68

NATO AUTHORITIES	
Defence Planning Committee	3
NAMILCOM	2
SACLANT	10
SACLANTREPEUR	1
CINCWESTLANT/COMOCEANLANT	1
COMSTRIKFLTANT	1
COMIBERLANT	1
CINCEASTLANT	1
COMSUBACLANT	1
COMMAIREASTLANT	1
SACEUR	2
CINCNORTH	1
CINCSOUTH	1
COMNAVSOUTH	1
COMSTRIKFORSOUTH	1
COMEDCENT	1
COMMARAIRMED	1
CINCHAN	3

SCNR FOR SACLANTCEN	Copies
SCNR Belgium	1
SCNR Canada	1
SCNR Denmark	1
SCNR Germany	1
SCNR Greece	1
SCNR Italy	1
SCNR Netherlands	1
SCNR Norway	1
SCNR Portugal	1
SCNR Turkey	1
SCNR U.K.	1
SCNR U.S.	2
SECGEN Rep. SCNR	1
NAMILCOM Rep. SCNR	1

NATIONAL LIAISON OFFICERS	
NLO Canada	1
NLO Denmark	1
NLO Germany	1
NLO Italy	1
NLO U.K.	1
NLO U.S.	1

NLR TO SACLANT	
NLR Belgium	1
NLR Canada	1
NLR Denmark	1
NLR Germany	1
NLR Greece	1
NLR Italy	1
NLR Netherlands	1
NLR Norway	1
NLR Portugal	1
NLR Turkey	1
NLR UK	1

Total initial distribution	248
SACLANTCEN Library	10
Stock	22
Total number of copies	280